ESTIMATION OF RECEIVER SAMPLING CLOCK TIMING IMPURITY IMPACT ON CHANNEL ORTHOGONALITY IN OFDM BASED COMMUNICATION SYSTEMS

A THESIS

SUBMITTED TO THE DEPARTMENT OF ELECTRICAL AND

ELECTRONICS ENGINEERING

AND THE INSTITUTE OF ENGINEERING AND SCIENCES

OF BILKENT UNIVERSITY

IN PARTIAL FULFILLMENT OF THE REQUIREMENTS

FOR THE DEGREE OF

MASTER OF SCIENCE

By

H. Onur TANYERİ

August 2009

I certify that I have read this thesis and that in my opinion it is fully adequate, in scope and in quality, as a thesis for the degree of Master of Science.

Dr. Tarık REYHAN(Co-Supervisor)

I certify that I have read this thesis and that in my opinion it is fully adequate, in scope and in quality, as a thesis for the degree of Master of Science.

Prof. Dr. Erdal ARIKAN(Co-Supervisor)

I certify that I have read this thesis and that in my opinion it is fully adequate, in scope and in quality, as a thesis for the degree of Master of Science.

Assist. Prof. Defne AKTAŞ

I certify that I have read this thesis and that in my opinion it is fully adequate, in scope and in quality, as a thesis for the degree of Master of Science.

Assist. Prof. F. Ömer İlday

Approved for the Institute of Engineering and Sciences:

Prof. Dr. Mehmet Baray
Director of Institute of Engineering and Sciences

ABSTRACT

ESTIMATION OF RECEIVER SAMPLING CLOCK TIMING IMPURITY IMPACT ON CHANNEL ORTHOGONALITY IN OFDM BASED COMMUNICATION SYSTEMS

H. Onur TANYERİ
M.S. in Electrical and Electronics Engineering
Co-Supervisor: Prof. Dr. Erdal ARIKAN
Co-Supervisor: Dr. Tarık REYHAN
August 2009

The growing need for high-speed wireless communication systems has led communication engineers to design and implement communication systems at higher frequencies where more bandwidth is available, use digital modulation schemes with more complex constellations and place carriers closer together with little guard-band in the pursuit of designing communication systems closer to the channel capacity. These new designs have placed tighter constraints on the performance of oscillators and timing devices of transceivers. In this work, the effects of timing clock jitter on the receiver Analog-to-Digital Converter (ADC) of Orthogonal Frequency Division Multiplexing (OFDM) based communication systems are examined and Inter-Carrier Interference (ICI) effects are quantified in order to prevent unnecessary over designs in OFDM ADC circuitry. In this respect, a simulation tool that synthesizes jitter processes with defined spectral characteristics is prepared. The generated jitter processes are utilized in an OFDM simulation tool that quantifies the ICI levels caused by receiver ADC

sampling jitter. Using these two tools, ICI levels of certain OFDM systems are examined and guidelines for OFDM ADC circuitry design are proposed.

Keywords: Phase Noise, Phase Noise Synthesis, Jitter, ADC Sampling Jitter, Orthogonal Frequency Division Multiplexing (OFDM), Inter-Carrier Interference (ICI)

ÖZET

ALMAÇ ÖRNEKLEME ZAMANLAMA HATALARININ OFDM HABERLEŞME SİSTEMLERİNDEKİ KANAL ORTOGONALİTESİNE ETKİSİNİN TAHMİNİ

H. Onur TANYERİ
Elektrik ve Elektronik Mühendisliği Bölümü Yüksek Lisans
Ortak Tez Yöneticisi: Prof. Dr. Erdal ARIKAN
Ortak Tez Yöneticisi: Dr. Tarık REYHAN
Agustos 2009

Yüksek hızlı kablosuz haberleşme sistemlerine artan talep ve ihtiyaç haberleşme mühendislerini daha fazla bant genişliğinin bulunduğu yüksek frekanslarda haberleşme sistemleri tasarlayıp yapmaya, daha karmaşık modülasyon şemaları kullanmaya ve frekans çoklamalı sistemlerde bilgi barındıran taşıyıcıların frekanslarını birbirlerine daha yakın koymaya zorlamıştır. Bu yeni tasarım gereksinimleri almaç ve göndermeçlerdeki osilatör ve zamanlama elemanları üzerine yeni performans kısıtlamaları getirmiştir. Bu çalışmada Ortogonal Frekans Çoklamalı (OFDM) temelli haberleşme sistemlerindeki almaçların Analog Dijital Çeviricilerinin (ADC) örnekleme zamanlarındaki titreşmelerin OFDM temelli haberleşme sistemlerine etkileri incelenmistir. Bu inceleme sayesinde bahsedilen bu etkilerin büyüklükleri belirlenerek OFDM almaç devrelerinde yapılan aşırı sıkı tasarımlar engellenebilir. Bu etkilerin belirlenmesi için öncelikle belirli tayf yoğunluk karakteristiklerine sahip örnekleme zamanlaması titreşme sinyallerini sentezleyebilen bir program hazırlanmıştır. Bu programın çıktı sinyalleri çesitli OFDM sistemlerini simüle edebilen bir programın almaç örnekleme

saatinde kullanılarak bu titreşmelerin kanal ortogonalitesine olan etkileri ve yarattıkları Taşıyıcılar Arası Enteferans (ICI) seviyeleri simülasyonlarla belirlenmiştir. Belirlenen bu seviyeler temel alınarak OFDM almaç ADC tasarımında kullanılabilecek öneriler sunulmuştur.

Anahtar Kelimeler: Faz gürültüsü, Zamanlama titreşmesi, Analog Dijital Çevirici, örnekleme zamanı titreşmesi, Ortogonal Frekans Çoklamalı Haberleşme Sistemleri (OFDM), Taşıyıcılar Arası Enteferans (ICI)

ACKNOWLEDGMENTS

I would like to thank my father İbrahim TANYERİ, my mother Ergül TANYERİ and my sister Başak TANYERİ for supporting me all my life. Their presence is a blessing.

I would also like to thank all of my teachers and professors for enlightening me and helping me discover the beauty of engineering. I would especially like to thank Dr. Tarık REYHAN for bearing with me for the last three years and constantly teaching me through this time.

I would also like to thank my Co-supervisor Prof. Dr. Erdal ARIKAN for all of his efforts. Especially for helping me understand the methodology in scientific research.

Last, but not least, I would like to thank all of my friends Anıl BAYER, Ceyda BAYER, And SÜREKCİGİL, Barbaros ŞERBETÇİ, Sıla KURAL and my colleagues at Biluzay that encouraged and helped me constantly.

Contents

List of Figures

List of Tables

Dedicated to My Family

Chapter 1

Introduction

The electromagnetic spectrum is a very valuable and scarce resource. The ever increasing need for high-speed wireless communication systems has caused the electromagnetic spectrum to get crowded with information bearing carriers. This situation has forced communication engineers to design communication systems at higher frequencies where more bandwidth is available. Still, the availability of new frequency bands in the spectrum, if not protected by regulations, is destined to get crowded. This fact indicates the need to maximally utilize the electromagnetic spectrum. This can be done by designing bandwidth efficient wireless communication systems that can operate close to the channel capacity. This means, placing carriers close together in frequency division multiplexed systems and using complex digital modulation schemes in order to transmit at higher data rate using small bandwidths. By performing the actions mentioned above, one can make better use of the spectrum. These actions place some constraints on certain parameters of communication systems. One set of constraints is placed on timing devices of wireless transceivers. Parameters like phase noise, jitter and stability that define the purity of oscillators are closely related to these constraints. These challenges in the design can be overcome by various expensive solutions with excessive designs, such as using over qualified components

in the design, like unnecessarily stable oscillators with unnecessarily low phase noise performance. But the telecommunication market favors cheap, simple and lightweight(mobile) systems that consume less power.

In this work, Orthogonal Frequency Division Multiplexing (OFDM) based communication systems which are highly bandwidth efficient communication systems are investigated. OFDM is being increasingly used as standard digital multi-carrier modulation method in various communication systems due to its bandwidth efficient nature and its robustness against multipath effects. The bandwidth efficient nature of OFDM comes from the fact that channel filtering (selection) is done by the orthogonality of the OFDM carriers. OFDM systems do not require guard-band. Furthermore, OFDM channels spectrally overlap in the frequency domain. This kind of spectral efficiency comes with its cost. OFDM communication systems are highly vulnerable to synchronization errors. This vulnerability results in stringent requirements for the timing elements of OFDM communication systems. The impact of these constraints should be quantified and converted into design specifications for efficient designs.

In this thesis, the focus is on the effects of receiver ADC sampling clock timing jitter on OFDM communications. In the thesis a perfect channel is assumed, only the timing jitter on the receiver sampling clock is considered as an impurity (i.e impurities like quantization noise, ADC aperture jitter are not included in the analysis). The amount of Inter-Carrier Interference (ICI) caused by timing jitter in OFDM receiver ADC's is quantified for various OFDM communication systems. For this purpose jitter processes are modelled and generated. The generated processes are used in MATLAB simulations and ICI levels in OFDM carriers have been quantified for various OFDM communication systems. This thesis builds up on the following five parts:

In Chapter 2, OFDM communication systems and the fundamental properties of OFDM are examined. The principles of OFDM communication systems are presented. OFDM parameters and OFDM parameters that are important for the analysis of receiver ADC sampling jitter effects are stated. Lastly, the effects of certain timing impurities on OFDM systems has been investigated.

In Chapter 3, oscillator fundamentals, oscillator parameters and timing impurities on oscillators are examined. Phase noise is studied in detail, because phase noise will be used extensively in the analysis. The definition of phase noise, the sources of phase noise, factors adding onto phase noise, ways of modelling phase noise, the relation between oscillator phase noise and timing jitter are presented.

In the Chapter 4 a summary of the previous studies performed on ICI created by local oscillator phase noise and ICI created by the timing jitter of the oscillator driving the receiver ADC of the OFDM receiver is presented. First, the previous work on the ICI effects caused by the phase noise of local oscillators performing frequency conversions are reviewed. Also, the techniques that are proposed for eliminating these effects are reviewed. Finally, the previous work on ICI caused by receiver ADC sampling clock timing jitter in OFDM systems is presented.

In Chapter 5, the analysis and studies performed on the ICI effects caused by OFDM receiver ADC sampling clock jitter are presented. First, the simulation tool that is prepared to generate jitter processes with defined phase noise spectrum is presented. Then, the model that is used for simulating the ICI effects created due to jitter is presented.

For quantifying the ICI caused by receiver ADC sampling jitter, Zero-IF transmitter and receiver structures which perform frequency conversions with a single

I, Q mixer are considered. The block diagrams of the OFDM transmitter and receiver that are used in the simulations are depicted in fig. 1.1 and fig. 1.2.

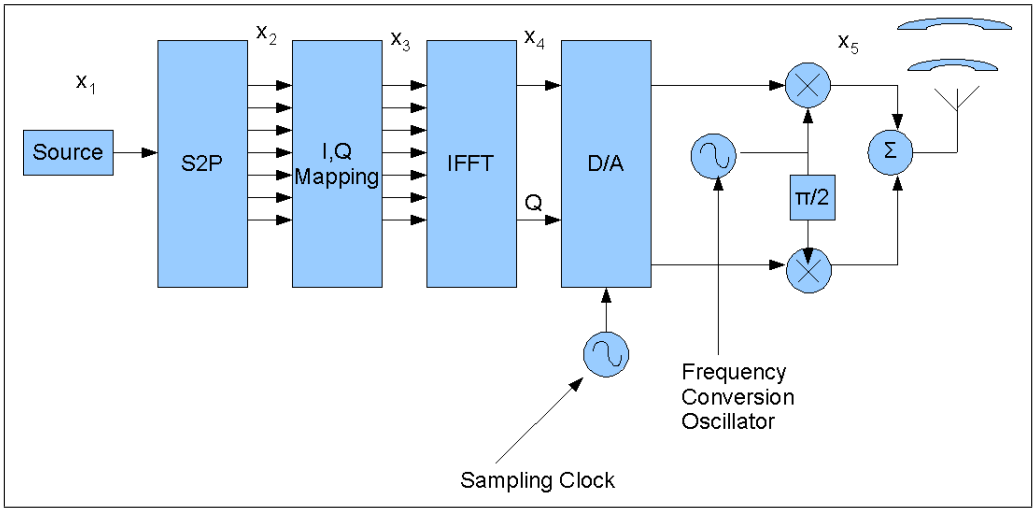

Figure 1.1: Zero-IF OFDM Transmitter Used in Simulations

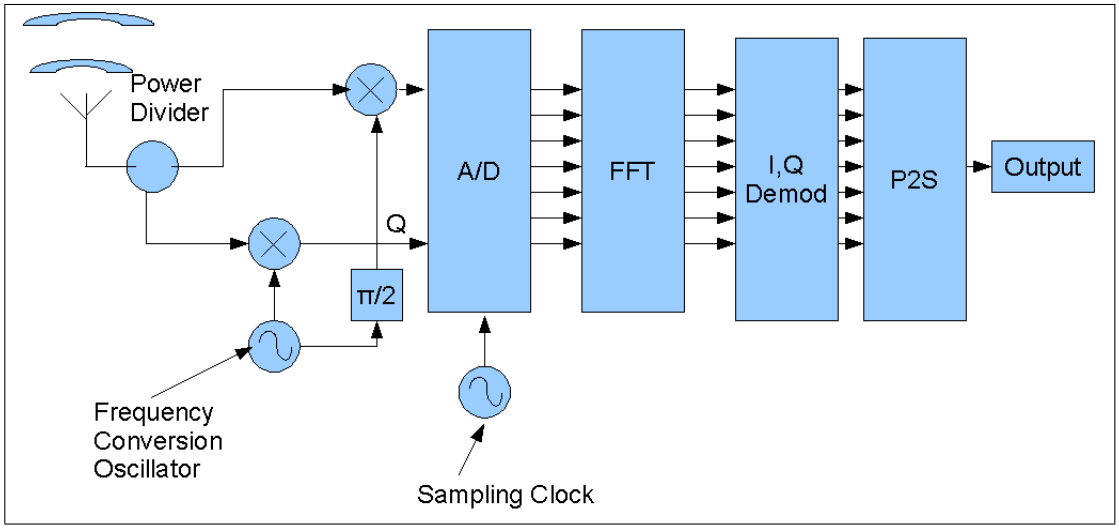

Figure 1.2: Zero-IF OFDM Receiver Used in Simulations

The OFDM communication equation that is used for simulating the ICI in the OFDM carriers is given in below. The derivation of this equation can be found in Chapter 5.

$$\tilde{x}[m] = \frac{1}{N} \sum_{k=-\frac{N}{2}}^{\frac{N}{2}-1} \sum_{n=-\frac{N}{2}}^{\frac{N}{2}-1} \left(x[n] e^{j2\pi \frac{(k+\zeta)(n-m)}{N}} \right) \tag{1.1}$$

In eqn. 1.1 $x[n]$ denotes the transmitted data, $\tilde{x}[m]$ denotes received data, k denotes the time normalized to the sampling period, n denotes the frequency normalized to the system bandwidth, ζ denotes the cumulative time jitter in sampling and N denotes the total number of carriers in the system.

Jitter processes generated by the aforementioned simulation tool are injected into the communication system through the ADC depicted in fig. 2.2. In generating jitter processes oscillators from different oscillator manufacturers are considered. The spectral qualities of the generated processes are matched to the information on the datasheets of the oscillators that are considered. For analysis, two communication systems using OFDM as a Digital Multi-Carrier modulation method is considered. Simulations are performed on sample IEEE 802.11a and 802.15.3a communication systems and the ratio of interference power to carrier power (I/C) in OFDM carriers are computed. These kinds of ratios are important in design of communication systems since, the maximum level of noise allowed in the system is distributed among sources of noise and interference. Thus, by quantifying the interference caused by sampling jitter in the receiver ADC the other parameters in the system can be chosen such that the maximum noise and interference level in the system is kept under the limits for desired communication quality.

Based on the results obtained from the simulations, discussions are presented on the effects of the sampling jitter in OFDM communication systems. These discussions provide information on the relations between certain OFDM system

parameters and the interference created due to sampling jitter with certain spectral distribution. Finally, some guidelines for the design of OFDM ADC circuitry are proposed.

In Chapter 6, the conclusions obtained from the studies and the simulations carried out were stated and the thesis is concluded by pointing out to future work that may be done to further investigate the effects of timing impurities on OFDM systems.

Chapter 2

OFDM As a Bandwidth Efficient Communication System

2.1 OFDM

In this chapter of this thesis, Orthogonal Frequency Division Multiplexed (OFDM) communication systems are examined as bandwidth efficient communication systems that are effected by receiver ADC sampling jitter. OFDM parameters and the parameters that are important for the analysis of ICI effects caused by receiver ADC sampling clock timing jitter are stated.

OFDM is a digital multi-carrier modulation method. It is a communication scheme that is being used increasingly in wireless communication systems. OFDM has been adopted as a standard multi-carrier modulation method in communication systems like IEEE 802.11a, 802.11g, HIPERLAN/2, ETSI DVB-T, WiMAX and many more. The reasons behind the widespread acceptance of OFDM are listed below;

- Bandwidth Efficiency: OFDM allows high datarate transmission in a bandwidth efficient manner.
- Robustness Against Multipath effects: OFDM are robust to multipath effects due to the fact that the low symbol rate in OFDM carriers
- Ease of Implementation: Modulation on orthogonal carriers can be easily implemented using FFT and IFFT operation

The fundamentals of OFDM operation, OFDM parameters, the advantages and disadvantages of OFDM are explained in the following parts of this chapter.

2.2 OFDM Fundamentals

The first study on OFDM dates back to 1966. Robert W. Chang of Bell Labs filed a U.S patent [6] that introduced the idea of dividing the transmission bandwidth into consecutive channels and modulating parallel datastreams on orthogonal carriers without guard-band, thus performing high data-rate transmission in a bandwidth efficient manner. The main idea of operation in OFDM communication systems is as follows;

The source (serial data) stream is divided into parallel lower data-rate substreams (channels) with equal datarates, then digital modulation (mapping the symbols to the I, Q plane) is performed on the parallel data substreams. Afterwards these modulated substreams are modulated with orthogonal carriers. On the receiver side, the received signal is demodulated using the same orthogonal carriers and digital demodulation is performed. Afterwards parallel datastreams (bit sequences) are demultiplexed (de-parallelized) into a single stream. These oprerations result in successful OFDM data communication. Figure 2.1 depicts a simple OFDM transmitter and fig. 2.2 depicts a simple OFDM receiver.

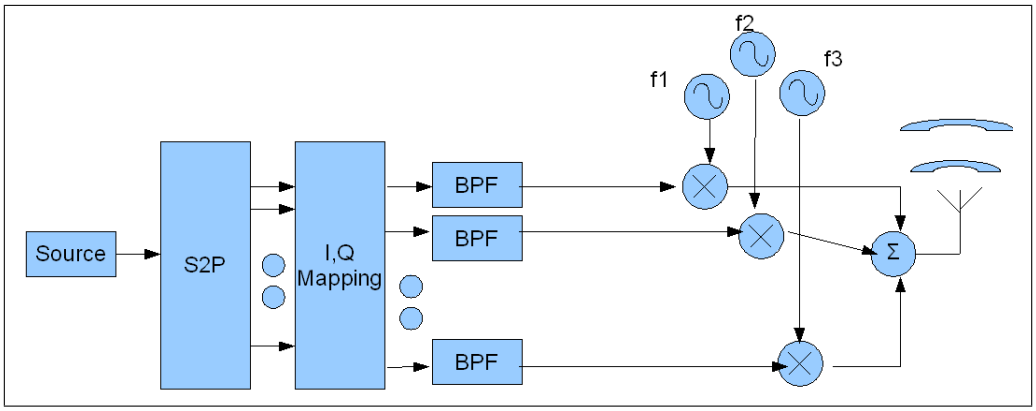

Figure 2.1: Simple OFDM Transmitter Block Diagram

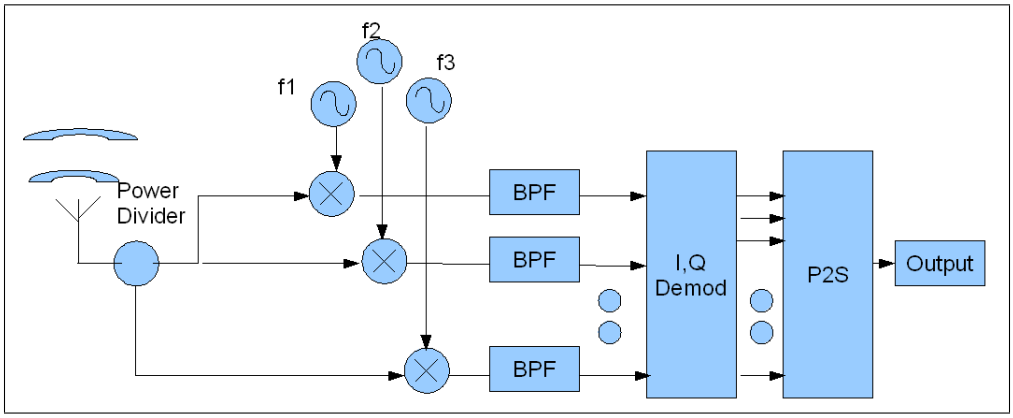

Figure 2.2: Simple OFDM Receiver Block Diagram

It is just to explain how OFDM communication systems work and state the conditions for zero Inter Symbol Interference(ISI) and zero Inter-Carrier Interference(ICI). In this respect the following part from the aforementioned patent [6] that explains zero ICI and zero ISI conditions for OFDM communication systems is presented.

Let c_n represent the digitally modulated symbols that will be transmitted through the i^{th} channel with $1/T$ symbol rate, $a_i(t)$ denote the impulse response

of the transmit filter of the i^{th} channel and $H(f).e^{j\phi(f)}$ denote the spectral response of the transmission media. The output of the i^{th} filter produces the following output sequence;

$$c_0 a_i(t), c_1 a_i(t-T), c_2 a_i(t-2T)..... \tag{2.1}$$

Thus the received sequence is as given below;

$$c_0 u_i(t), c_1 u_i(t-T), c_2 u_i(t-2T)..... \tag{2.2}$$

Where $u_i(t)$ is the combined impulse response of the channel and the transmit filter of the i^{th} channel.

$$u_i(t) = \int_{-\infty}^{\infty} h(t-\tau) a_i(\tau) d\tau \tag{2.3}$$

The received signal has no Inter Symbol interference (ISI) if the Nyquist zero ISI criterion is satisfied. Namely;

$$\int_{-\infty}^{\infty} u_i(t) u_i(t-kT) dt = 0, \forall k = \pm 1, \pm 2, ... \tag{2.4}$$

In order to show that OFDM channels do not interfere with each other a similar path is used and conditions for zero ICI is derived.

Let the j^{th} channel be another channel in the OFDM communication system. Similar to the i^{th} channel the received sequence at channel j is;

$$d_0 u_j(t), d_1 u_j(t-T), d_2 u_j(t-2T)..... \tag{2.5}$$

Where d_n's denote the symbols transmitted through channel j with symbol rate 1/T and u_j's denote the combined impulse response of the j^{th} bandpass filter and the channel. Thus;

$$u_j(t) = \int_{-\infty}^{\infty} h(t-\tau) a_j(\tau) d\tau = 0 \tag{2.6}$$

Although the symbols received from the i^{th} and the j^{th} channel overlap in time there will be no ICI if;

$$\int_{-\infty}^{\infty} u_i(t) u_j(t-kT) d\tau = 0, \forall k = 0, \pm 1, \pm 2, ... \tag{2.7}$$

Conditions given in eqn. 2.4 and eqn. 2.7 lead to information on the transmit filter characteristics. The Fourier transform of zero ISI criterion 2.4 states that the joint response of the transmit filter (with spectral representation $A_i(f)$) and the channel ($H(f)$) must satisfy the following spectral properties for zero ISI.

$$\int_0^{\infty} H^2(f) A_i^2(f) \cos(2\pi f k T) df = 0 \forall, k = \pm 1, \pm 2.... \tag{2.8}$$

The Fourier transform of the zero ICI conditions give the following information about the transmit filters of the channels.

$$\int_0^{\infty} H^2(f) A_i(f) A_j(f) \cos(\beta_i(f) - \beta_j(f)) \cos(2\pi f k T) df = 0, k = \pm 1, \pm 2.... \tag{2.9}$$

$$\int_0^\infty H^2(f)A_i(f)A_j(f)\sin(\beta_i(f)-\beta_j(f))\cos(2\pi fkT)df = 0, k = \pm 1, \pm 2.... \tag{2.10}$$

Where $\beta_i(f)$ and $\beta_j(f)$ denote the phase response of the i^{th} and j^{th} channels transmit filters. Filters satisfying these conditions are fit for OFDM communications.

In [8] a method is given find and design filters satisfying the aforementioned zero ISI and zero ICI conditions. This method is left out of this work. A Sample OFDM filter bank satisfying the aforementioned conditions is given in fig. 2.3.

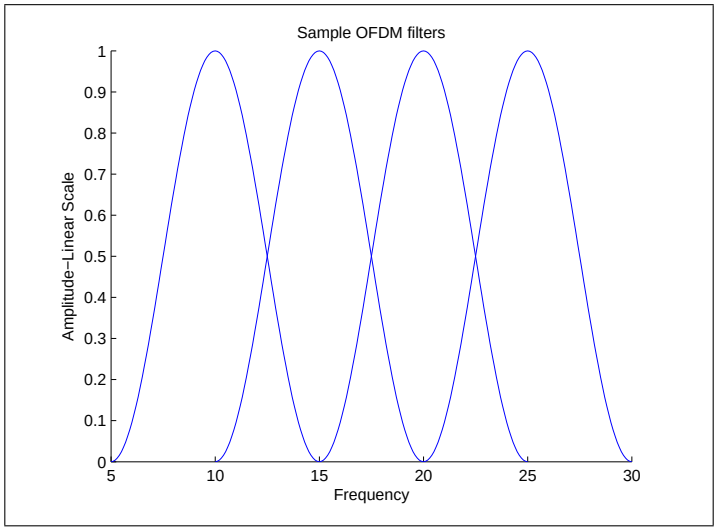

Figure 2.3: Sample Transmit and Receive Filters For an OFDM Communication System

In this filter family the i^{th} channel transmit filter is defined with the following frequency response.

$$A_i^2(f) = \frac{1}{2} + \frac{1}{2}\cos\left(\pi\frac{(f-f_i)}{2f_s}\right) \tag{2.11}$$

OFDM communication systems with carriers separated by frequency f_s (where $f_s = 1/T_s$ is the symbol rate of a single channel) are capable of performing data transmission at a symbol rate of $2f_s$ per OFDM carrier. This is a very bandwidth efficient communication system, since every carrier can carry the maximum symbol rate and spectral overlap can take place as depicted in fig. 2.3. This is possible due to the orthogonality of OFDM carriers. This is, one of the many advantages of OFDM communication systems. Another advantage of OFDM is its robustness against frequency selective channel effects. Since the total bandwidth is divided (distributed) among carriers, the frequency selective fading will only effect certain carriers. These effects could be dealt with, by using relatively simple equalizers at the receiver. This property is very desirable to have, especially in systems with high bandwidth because it reduces the complexity of the OFDM receiver.

Another reason for OFDM to be a widely used multi-carrier modulation method is due to the ease of implementation. The modulation of substreams onto orthogonal carriers and the filtration which enables the spectral efficiency of OFDM can be implemented by an IFFT (Inverse Fast Fourier Transform) operation at the transmitter and a FFT (Fast Fourier Transform) operation at the receiver. The advances in microprocessor technologies enables high data-rate OFDM systems to be implemented with a single microprocessor. OFDM carriers generated from an IFFT operation is depicted in the frequency domain in fig. 2.4 and in time domain in fig. 2.5.

OFDM has its disadvantages as well. The orthogonality property of OFDM that enables OFDM to be a bandwidth efficient communication system causes OFDM systems to be very vulnerable to synchronization errors. Due to the fact that neighbouring channel rejection (filtering) depends only on orthogonality, any synchronization error effecting the orthogonality of OFDM carriers causes

leakage through (and between) the OFDM channels. These leakages result in quick decreases in the the Signal to Noise Ratio (SNR) in OFDM channels, leading to an increase in Bit Error Rate (BER).

Another disadvantage of OFDM communication systems is that they require very linear amplifiers. The crest factor (Peak Power to Average Power ratio) in OFDM systems can get very high. This is possible, since symbols on different carriers can align in phase and cause very large signal levels that can push the power amplifiers at OFDM transmitters to saturation. The crest factor depends on the number of carriers and the type of constellation mapping used in the system. In OFDM systems crest factors can go as high as 12 dB [30]. This systems require highly linear power amplifiers and high back-off values in OFDM transmitters.

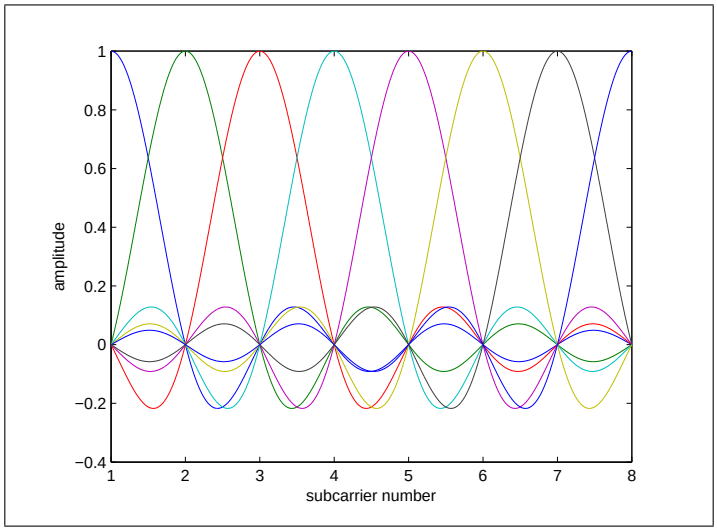

Figure 2.4: OFDM Filters Created by IFFT Operation For an Eight Channel OFDM System(Frequency Domain)

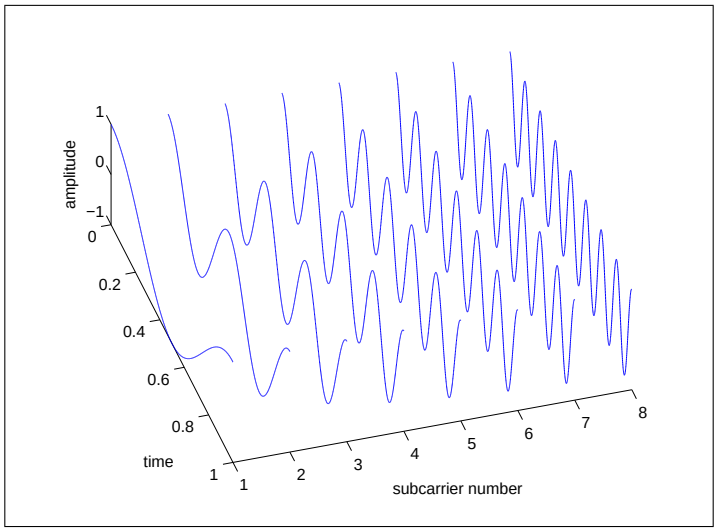

Figure 2.5: OFDM Filters Created by IFFT Operation For an Eight Channel OFDM System(Time Domain)

In order to carry out the analysis, OFDM communication equations must be derived using the communication system that is assumed. In this thesis, a typical OFDM communication system with zero-IF architecture using a IFFT for the multi-carrier modulation and FFT as the multi-carrier demodulation method is considered. Figure 2.6 depicts such a transmitter using IFFT for multi-carrier modulation and fig. 2.7 depicts the matching receiver.

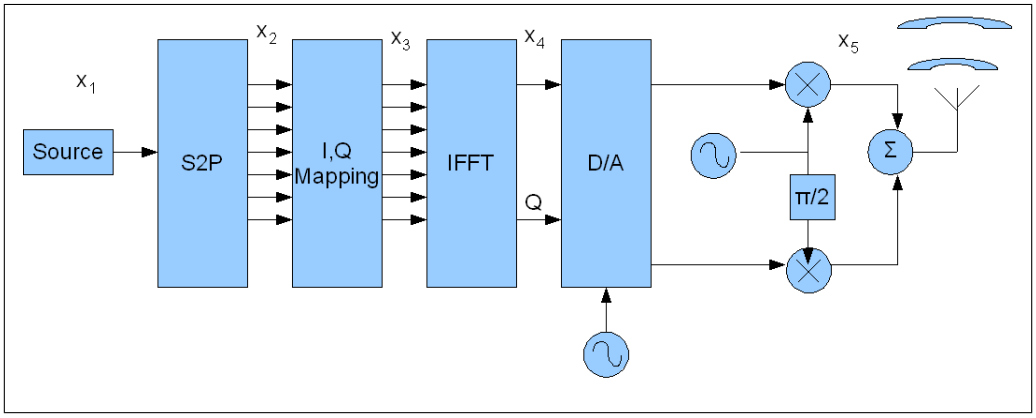

Figure 2.6: Block Diagram of an OFDM Transmitter Using IFFT For Multi-Carrier Modulation

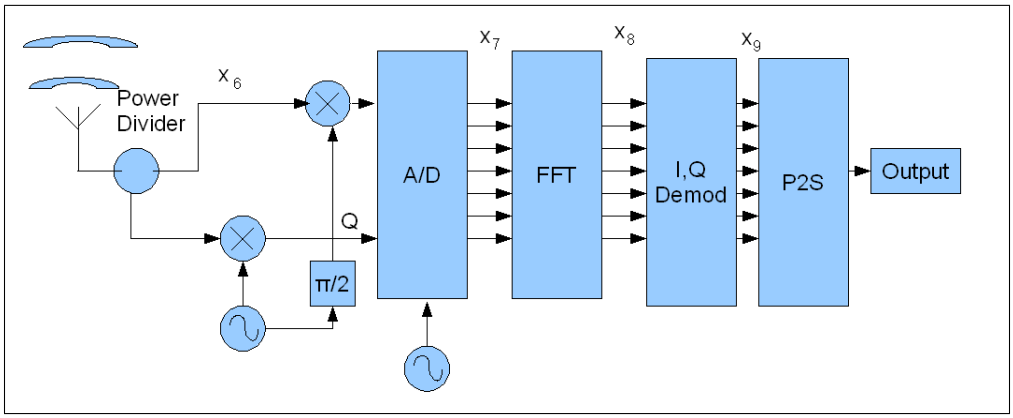

Figure 2.7: Block Diagram of an OFDM Receiver Using FFT For Multi-Carrier Demodulation

The signals and the operations on the signals through the marked nodes on the block diagrams are explained below;

The input datastream consisting of a bit sequence will be parallelized according to the number of parallel channels in the system. In an N-channel OFDM communication system, if the input consisting ofof N symbols is denoted by $\vec{x_1}$ the signal at x_2 is $x_2 = \vec{x_1}^t$, meaning the input symbol stream is parallelized. In short, the 1 by M stream is multiplexed into N by M/N substreams throughout serial to parallel converter.

After the datastream is parallelized, the digital modulation(constellation mapping) is performed. The order of multiplexing and constellation mapping operations can be interchanged. At node x_3 N substreams consisting of complex symbols on the I, Q plane are present.

Multiplication with the complex exponents in the IFFT operation results in modulation onto orthogonal carriers. The mathematical formulation is shown below;

$$X[k] = \sum_{n=-\frac{N}{2}}^{\frac{N}{2}-1} x[n] e^{j2\pi kn/N} \tag{2.12}$$

In eqn. 2.12, k denotes the time index normalized to the symbol period T_s, n denotes the frequency index normalized to the symbol rate f_s and N denotes the total number of carriers in the communication system. Notice that IFFT operation with the complex multiplication operations corresponds modulating the low datarate substreams onto orthogonal frequencies with frequency index n. The real and imaginary components of the IFFT output are separated into I and Q components for frequency upconversion.

After the substreams are modulated onto orthogonal carriers, they are input to Digital to Analog Converter(DAC) and frequency upconversion is performed at x_5 with an I, Q mixer and a local oscillator. The output of the transmitter is given in eqn. 2.13.

$$s(t) = \frac{1}{\sqrt{N}} \sum_{n=-\frac{N}{2}}^{\frac{N}{2}-1} (x[n] e^{j2\pi kn/N}) e^{j\omega_{tr} t} \tag{2.13}$$

The signal detected at the receiver antenna x_6 undergoes I, Q frequency down-conversion using two oscillator signals locked in 90 deg phase and an I, Q mixer. The resulting I and Q signals are digitized using a ADC. At x_7 the frequency downconversion is completed and the orthogonally modulated carriers are at baseband.

The digitized I and Q signals are input to a processor and FFT is performed on these signals. Afterwards the complex symbols on the I, Q plane are de-mapped onto parallel bit sequences. After x_9, bit sequences are demultiplexed(serialized) and after the parallel to serial conversion the data transmission is complete. The formula at the output of the receiver is given eqn. 2.14 the simplified version of the equation is given in eqn. 2.15.

$$\tilde{x}[m] = \frac{1}{N} \sum_{k=-\frac{N}{2}}^{\frac{N}{2}-1} \sum_{n=-\frac{N}{2}}^{\frac{N}{2}-1} (x[n] e^{j2\pi kn/N}) e^{-j2\pi km/N} e^{j\omega_{tx}t} e^{-j\omega_{rx}t} \tag{2.14}$$

$$\tilde{x}[m] = \frac{1}{N} \sum_{k=-\frac{N}{2}}^{\frac{N}{2}-1} \sum_{n=-\frac{N}{2}}^{\frac{N}{2}-1} (x[n] e^{j2\pi k(n-m)/N}) e^{j(\omega_{tx}-\omega_{rx})t} \tag{2.15}$$

In 2.15, k denotes the time index normalized to T_s, n denotes the frequency index on the transmitter side normalized to the symbol period f_s, m denotes the frequency index on the receiver side normalized to the carrier spacing, N denotes the total number of carriers in the system, ω_{tx} and ω_{rx} denote the radial frequencies of the frequency conversion oscillators at the transmitter and receiver respectively.

In order to understand how the communication system works one can examine eqn. 2.15. It can be seen that the output $\tilde{x}[m]$, is equal to the input $x[n]$ when $n = m$ and $\omega_{tx} = \omega_{rx}$. Note that if $n \neq m$ and $\omega_{tx} = \omega_{rx}$, $\tilde{x}[m] = 0$. This means, there is no Inter-Carrier Interference from carrier n to carrier m. This condition is actually a discrete equivalent of the zero ICI condition given in eqn. 2.7.

Note that receiving the transmitted signal correctly highly depends on the orthogonality of carriers. If $\omega_{tx} \neq \omega_{rx}$ or there is some frequency errors during the FFT or IFFT operations the carriers will quickly leak into each other causing Interference in neighbouring carriers. These kinds of errors are named as frequency offsets. These errors can be dealt with using carrier recovery methods, [15],[20] gives details on several carrier recovery algorithms.

The basic idea behind carrier recovery relies on estimating the frequency offset between transmit receive signals and compensating for these offsets. This compensation is done by de-rotating the I, Q (constellation) plane with the offset frequency between the transmitter and the receiver.

Estimation of the frequency offsets are generally done with OFDM pilot signals. Pilot signals are signals with known content that are transmitted through certain OFDM carriers. At OFDM receivers, the degradation on the pilot signals are used as observations to estimate the effects of the transmission medium on the OFDM carrier. Pilot signals can be also used to compensate for the ICI effects caused by the phase noise of the local oscillators performing frequency conversion. This effect and some mitigation techniques are presented in Chapter 4.

Even if there are no frequency offsets between carrier frequencies of the transmitter and the receiver (meaning they synchronized in terms of frequency), there may be rapid fluctuations in the phase that cause the carrier spectrum to broaden and degrade the orthogonality of OFDM carriers. Also, even if there are varying timing errors between the transmitter and receiver, the orthogonality of carriers will not be met. The varying phase difference in the oscillator is caused phase noise of the oscillator and the varying timing drifts is caused by timing jitter in sampling instants. The effect of these impurities on OFDM will be presented in Chapter 4. These rapid fluctuations in the phase and timing do not degrade

the SNR in OFDM carriers as much as frequency offsets but these effects are bottlenecks[27] for efficient communication and they need to be quantified for efficient designs.

2.3 OFDM Parameters

In this section, the OFDM system parameters are stated. The fundamental parameters of an OFDM system are listed below;

- System Bandwidth: Total bandwidth in which data transmission occurs. The unit for bandwidth is Hertz (Hz).
- Symbol Rate: Total symbol rate carried over the bandwidth. The unit for Symbol rate is symbols per second.
- Data Rate: The data rate carried over the communication system. This value depends on the type of constellation mapping used in the system. For a data communication system using 4-QAM data rate is double the symbol rate. The unit for data rate is bits per second.
- FFT Size: The total number of carriers in the system.
- Effective Number Of Carriers: The number of carriers excluding the number of unused carriers and pilot carriers in the system.
- Cyclic Prefix or Guard Time: In the beginning of an OFDM symbol, a certain portion from the end of the same symbol is placed. This is to prevent Inter Symbol Interference due to multipath effects and the value of this parameter depends on the delay spread of the environment. The unit for guard time is seconds.
- Channel Spacing: The separation between two OFDM carriers. The unit for carrier spacing is Hertz.

From the parameters given above the parameters that are important for the analysis in this thesis are the total number of carriers, bandwidth and digital modulation type.

In this chapter OFDM based communication systems were examined. OFDM properties and fundamentals of OFDM communication systems were presented. The informative background presented here will be used for analyzing the effects of receiver ADC timing jitter on OFDM communication systems.

Chapter 3

Oscillator Fundamentals and Timing Impurities of Oscillators

3.1 Oscillator Fundamentals

An oscillator is an electronic circuit that outputs a periodic waveform with determined frequency. The output has a certain amplitude, frequency and phase. Oscillators are used as timing elements in electronics systems. They are key elements in frequency conversion applications along with mixers. They also provide timing information to various digital components. A typical oscillator block diagram is given in fig. 3.1

An oscillator consists of a frequency selective element (resonator), an active device (amplifier), an amplitude limiting mechanism and a positive feedback from the output to the input. The oscillator depicted in fig. 3.1 works as explained below;

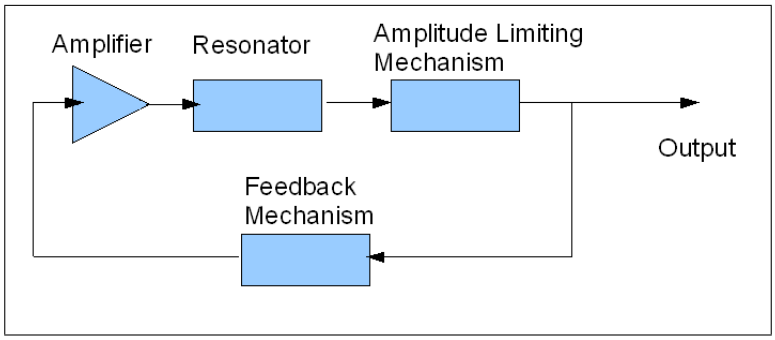

Figure 3.1: Typical Oscillator Block Scheme

The thermal noise inherent in the system is amplified by the amplifier. The resonator filters out the undesired frequency components in the signal and the positive feedback mechanism creates instability in the system causing the system to output a signal with increasing amplitude. Certain amplitude limiting mechanisms are placed in the oscillators to control the amplitude of the oscillation. Thus the oscillator outputs a signal with certain amplitude at steady-state. The frequency content of the output signal is determined by the characteristics of the resonator.

If the feedback mechanism is not set properly, the depicted oscillator is essentially a (frequency) tuned amplifier. There exists a condition to guarantee the oscillation. This condition is known as the Barkhausen oscillation condition[12]. This condition essentially states, the need for an unstable loop to create a growing signal which reaches to a stable amplitude after the transient effects wear out.

The oscillator parameters that can be found on a datasheet are listed below;

- Frequency of oscillation: Defines the center frequency of the resonator used in the oscillator. The unit for this parameters is Hz.
- Output signal strength: Defines the output power of the oscillator. The unit for this parameter is dBm(power) or volts (voltage).

- Tuning: If the resonator of the oscillator can be tuned in a certain frequency range the oscillator is said to be tunable. Tunable oscillators are very widely used in communication systems. The unit for this parameter is Hz.

- Frequency stability: Oscillation frequency of an oscillator tends to drift with time. There are many reasons for the oscillation frequency to drifts. Some examples causing frequency drift are; temperature changes in the system, the effect of ageing in various components of the oscillator, microphonic (vibration based) effects etc. The units for frequency stability is given ppm(parts per million). For example, the frequency stability of a crystal oscillator could be given as ± 1 ppm in the temperature range $-40 + 85°C$. This would mean an oscillators central oscillation frequency will deviate from its central oscillation frequency by a fraction of 10^{-6} (i.e if the oscillator has central oscillation frequency of 10 MHz, 1 ppm drift would result in 10Hz frequency drift causing the oscillator to oscillate at a frequency of 10MHz $\pm$ 10 Hz.

- Frequency push: The variations in the supply voltages cause the resonator center frequency to change resulting in a drift in the oscillation frequency, the amount of frequency drift caused by supply voltage variation is called frequency push. The unit for frequency push is Hz/Volts.

- Frequency pull: The variations on the load of the oscillator loads the resonator and causes frequency drifts in the center frequency of oscillation. The frequency drift, caused by loading, is named as frequency pull. The unit for frequency pull is Volts/Ω.

- Phase noise: Phase noise is a parameter defining the spectral purity of the oscillator, it is closely related to the wandering in the phase of oscillation. The unit for phase noise is dBc/Hz.

In this thesis, the focus is mainly on short term non-static impurities on the phase of oscillators. This does not mean that other impurities are not important in OFDM systems. On the contrary, the orthogonality is drastically effected by all sorts of synchronization errors, such as frequency offsets and drifts in central oscillation frequency. These topics are well studied and these problems can be handled with carrier recovery algorithms. Some studies on carrier recovery algorithms are given in [15],[20]. Also, frequency offsets in oscillators due to ageing and temperature changes are processes that are relatively slow processes. These impurities can be considered as frequency offsets. The frequency drifts due to power supply and load instabilities can be decreased by providing isolation to the resonator from the source and the load as much possible. However, phase noise is not so easily handled. The rest of this chapter focuses on, phase noise and jitter as oscillator impurities and presents models for these impurities.

3.2 Phase Noise and Phase Noise Definition

The phase noise of an oscillator is a spectral quantity describing the purity of an oscillator and the short time fluctuations in the phase of oscillation. These kinds of timing impurities (along with frequency offsets) cause Inter-Carrier Interference(ICI). These effects cannot be dealt with, by using carrier recovery methods.

The output of an ideal oscillator is expected to be a pure sinusoidal. The output of the ideal oscillator is in the following form;

$$v(t) = A_v \cos(2\pi f_{osc} t + \phi) \tag{3.1}$$

Where, A_v denotes the amplitude of oscillation, f_{osc} denotes the frequency of oscillation and ϕ denotes the phase of the oscillation. This oscillator output corresponds to a pure dirac-delta function in the frequency domain. Figure 3.2 demonstrates the output of an ideal oscillator in time and frequency domain.

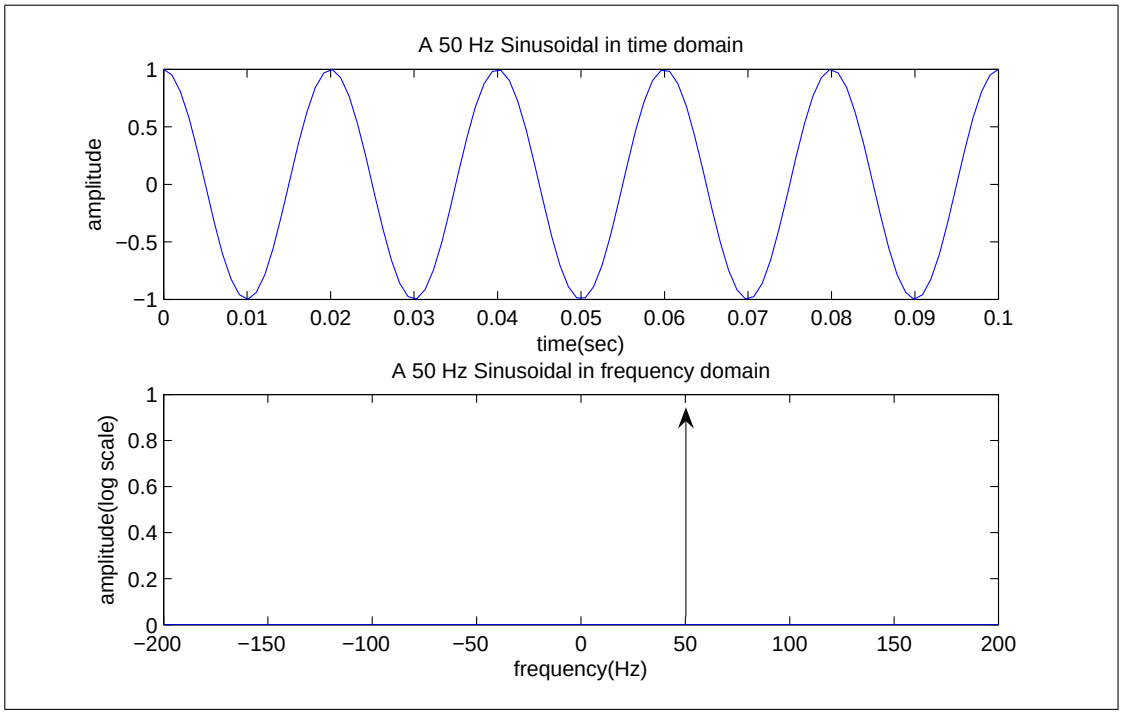

Figure 3.2: Output of an Ideal Oscillator

However, real oscillators have all kinds of impurities. The amplitude of oscillation, A_v may have some randomness. There may be drifts in f_{osc}, the frequency of oscillation and random phase fluctuations in $\phi(t)$ may be observed at the output of the oscillator. All of the mentioned impurities, may be caused by intrinsic effects or caused by external perturbations. In any case they, will degrade the purity of the oscillator and limit the performance of the communication system. Figure. 3.3 depicts an example for the output of an oscillator with impurities.

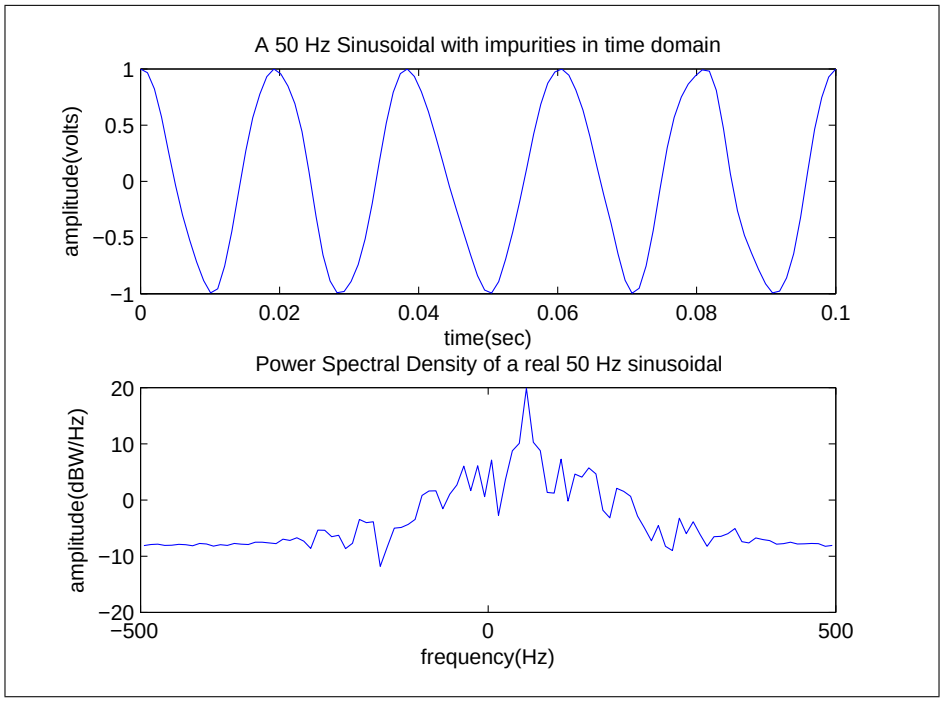

Figure 3.3: Output of a Real Oscillator

In early studies, phase noise was defined as follows;

For an oscillator with central oscillation frequency, f_{osc}, phase noise at frequency $f_{osc} + \Delta f$ is the ratio of the power measured at $f_{osc} + \Delta f$ (in one hertz bandwidth), to the total power of the carrier.

This definition is ambiguous, because it includes the spectral broadening due to other effects, such as amplitude noise. Later, a phase noise definition was given by IEEE standard 1139-1999. This definition isolated phase and amplitude noise in oscillators. This standard defines phase noise using the power spectral density of the phase function in the oscillation $S_\phi(f)$. According to this standard the phase noise at frequency $f_{osc} + \Delta f$ is defined as; half of the power level in one Hz bandwidth measured at offset frequency $f_{osc} + \Delta f$ [22]. Phase noise has units of dBc/Hz. Figure 3.4 depicts a sample phase noise plot for an oscillator.

The mathematical expression for the definition of phase noise is given in eqn. 3.2;

$$L(f_{osc} + \Delta f) = \frac{1}{2} S_{\phi}(f_{osc} + \Delta(f)) \tag{3.2}$$

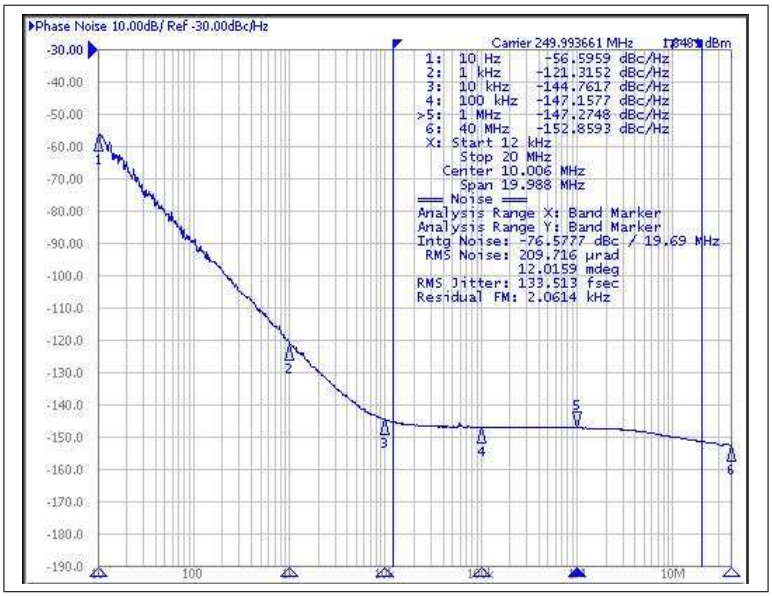

Figure 3.4: Sample Phase Noise Plot of an Vectron VCC6-QCD-250M000 Oscillator [31]

3.3 Phase Noise Models

In order to examine a system one has to develop and assume some models for the elements in the system (i.e assuming small signal models for analyzing amplifier blocks or assuming a noise source and noiseless elements to perform noise analysis). In order to understand the effects of phase noise on communication systems, a model must be assumed and used in the analysis.

Phase noise is often modelled as a Wiener random process (Brownian motion). This means that the phase of an oscillator performs a random walk with time. It will be just to mention, the main properties of a Wiener random process. The main properties of Wiener random processes are listed below;

- $W_0 = 0$, starting point of the process is zero by definition.
- The wandering of the process is continuous.
- $E[W_t] = 0$ The mean of the Wiener process is zero.
- $E[W_t W_s] = min(t, s)$ this is the auto-correlation function of the Wiener random process. This implies that the phase wanders boundlessly as time passes.
- Increments of W_t on non overlapping intervals are independent.

This process is not a wide sense stationary process, meaning that the statistical properties (autocorrelation function) of the process cannot be expressed as a function of the time difference between delayed Wiener processes. It is not mathematically correct to mention a Power Spectral Density(PSD). This is one of the challenging parts of working with phase noise.

The wandering of the phase of an oscillator output is modelled by a random walk. The amount or strength of the phase noise on a particular oscillator output will be defined by certain parameters of the oscillator. Various models have been developed to model oscillator phase noise. In the following section, several oscillator phase noise models will be explained.

3.3.1 Oscillator Phase Noise Models

One of the earliest studies on oscillator phase noise modeling was published in 1966 by D. B. Leeson[2]. This study presents a model to determine the phase noise spectrum for oscillators. The model accounts for and builds up on the spectral characteristics of the resonator, the effective noise figure of the oscillator, the $1/f$ noise characteristics of the active device used in the oscillator and the signal level at the input of the oscillator active device. The phase noise model offered by this study is as below;

$$S_{\phi}(w_m) = \left[\frac{\alpha}{\omega_m + 2FkT/P_s}\right]\left[1 + (\frac{\omega_0}{2Q\omega_m})^2\right] \tag{3.3}$$

In this equation;

- α represents a constant determined by the $1/f$ noise corner of the active device,
- F is the noise figure of the active device used in the oscillator,
- k is the Boltzmann constant,
- P_s is the signal level entering the active device of the oscillator,
- $\omega_0$is the central oscillation frequency,
- Q is the quality factor of the resonator used in the oscillator,
- ω_m is the offset frequency at which phase noise is calculated,

This model provides intuition for designing low phase noise oscillators by stating the importance of the resonators spectral qualities (namely, the Q of the resonator) and $1/f$ noise on phase noise spectrum.

Another oscillator phase noise model is proposed in [3]. In this study, the authors assume a linear periodic-time variant model for the oscillator. This assumption depends on, the periodic nature of the oscillator and the time variant response of the oscillator to injected noise currents. An oscillator injected with noise at the peak of the oscillation does not create any phase error, but creates randomness in the amplitude. However, if noise is injected during the zero crossing of the oscillator causes the maximum phase error.

With the linear periodic time variant oscillator assumption, the study bisects the injected noise to phase noise conversion in two steps; first, they define the injected noise to phase transfer function.

$$h_\phi(t,\tau) = \frac{\Gamma(\omega_0\tau)}{q_{max}} u(t-\tau) \tag{3.4}$$

Where $\Gamma(x)$ denotes the Impulse Sensitivity Function (ISF), q_{max} is the maximum charge displacement across the capacitor and u(t) is the unit step function. This impulse response function represents the change of phase, in an oscillator, when an impulse current is injected at phase $\omega_o\tau$. Here it is just to explain the ISF denoted as $\Gamma(x)$. This function is a dimensionless, frequency and amplitude independent 2π periodic function which is named as the Impulse Sensitivity Function. The ISF gives information on the sensitivity of the oscillator to injected noise current at various phases. The calculation of this function is explained in detail in [3]. The output of the injected noise to phase transfer function will undergo a phase to voltage transformation and produce phase noise. The injected noise to phase noise conversion mechanism is simply the phase modulation of the output waveform. Figure 3.5 depicts the two step injected noise to phase noise conversion mechanism.

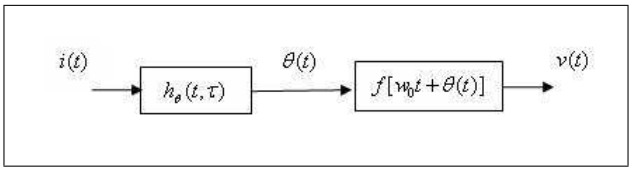

Figure 3.5: Injected Noise to Phase Noise Conversion Mechanism

By the help of the parameters above, the phase noise spectrum of an oscillator is characterized. For the $1/f^2$ region the phase noise spectrum is given by;

$$L(\Delta\omega) = 10log\left(\frac{\frac{\bar{i_n^2}}{\Delta f}\Gamma_{rms}^2}{4q_{max}^2\Delta\omega^2}\right) \tag{3.5}$$

Where i_n denotes the noise current ,Γ_{rms} is the rms value of the ISF.

For the $1/f^3$ region, the phase noise spectrum of the oscillator is given by

$$L(\Delta\omega) = 10log\left(\frac{\omega_{1/f}c_0^2\frac{\bar{i_n^2}}{\Delta f}}{8q_{max}^2\Delta\omega^3}\right) \tag{3.6}$$

Where i_n denotes the noise current c_0 denotes the first Fourier series expansion coefficient of the periodic ISF and $\omega_{1/f}$ is the 1/f corner frequency.

For further frequency offsets from the oscillation, the phase noise converges to the phase noise model proposed by Leeson.

This oscillator phase noise model adds improvements to the Leeson phase noise model through the calculation of the ISF and incorporating the $1/f^2$ and $1/f^3$ region of the phase noise spectrum. Modeling the oscillator nodes and calculating the ISF for this model takes some time but this model gives better accuracy on the phase noise (especially on close-in phase noise) of an oscillator.

The final oscillator phase noise model investigated in this thesis is the model by Demir et al.[5]. In this study, oscillator phase noise is examined rigorously without any assumptions(such as, high Q assumption for the resonator). This study performs a non-linear perturbation analysis and shows that orbital (amplitude) deviations remain small, for small perturbations, but the perturbations in the phase can grow unboundedly large with time. These findings fit the behaviour of phase noise in oscillators as the phase uncertainty in oscillators grows unboundedly with time. The variance of the phase uncertainty is modelled as linearly increasing.

After this analysis, the study characterizes the Probability Distribution Function (PDF) of phase noise and derives the power spectral density of an oscillator with phase noise.

$$S(\omega) = \sum_{i=-\infty}^{\infty} X_i X_i^* \frac{\omega_0^2 i^2 c}{\frac{1}{4}\omega_0^4 i^4 c^2 + (\omega + i\omega_0)^2} \tag{3.7}$$

Where X_i's denote the Fourier coefficients of the periodic unperturbed oscillation and c denotes the linear increase in the variance of the phase uncertainty in the phase of the oscillation.

The mentioned oscillator phase noise models are very useful for designing oscillators with low phase noise specifications, because they provide insight on the phase noise phenomenon and its sources in oscillators.

3.4 Jitter and Phase Noise to Jitter Conversion

In order to investigate the effect of Analog Digital Converter (ADC) sampling jitter, it will be useful to investigate jitter and phase noise to jitter conversion. The next section explains the jitter and jitter to phase noise conversion. Jitter is defined as the variations in the periodic behaviour of a signal. Jitter is measured by the RMS values of the deviation of the periodic signal from the ideal periodic signal. The units for jitter is given in seconds for time jitter and in radians for phase jitter. Figure 3.6 depicts the timing jitter in a sinusoidal signal.

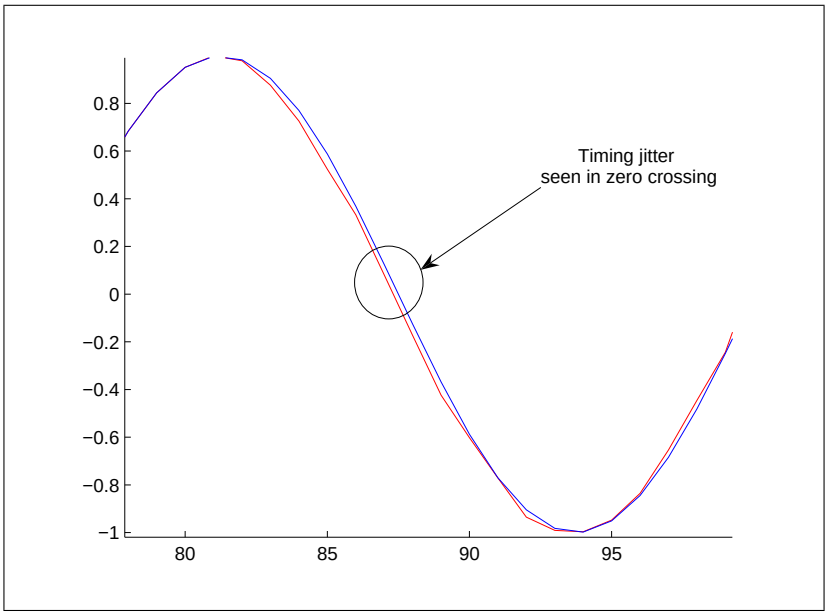

Figure 3.6: Illustration of Timing Jitter

The output of an oscillator and the component causing jitter should be examined, in order to derive a conversion from phase noise to timing jitter.

$$v(t) = A_v \cos(2\pi f_{osc} t + \phi(t)) \tag{3.8}$$

In eqn. 3.8, A_v denotes the amplitude of the oscillation and the argument of sinusiodal is the phase. Thus, the statistcs of $\phi(t)$ represent the phase jitter (deviation from the expected output phase) in radians. In order to find the timing jitter, the phase deviation should be divided by the radial frequency of oscillation namely, timing jitter $t_j = \frac{\phi}{2\pi f_{osc}}$. In order to find the rms power of jitter, the power spectral density of $\phi(t)$ should be integrated in the bandwidth of interest[26]. The expression for calculating rms power of phase jitter is given in eqn. 3.9 and for timing jitter rms power calculation is given in eqn. 3.10.

$$P_{pj} = \sqrt{\int_{BW} S_\phi(f)} \tag{3.9}$$

$$P_{tj} = \frac{1}{2\pi f_{osc}} \sqrt{\int_{BW} S_\phi(f)} \tag{3.10}$$

In this chapter, the fundamentals of oscillators and timing impurities on oscillators were presented. Furthermore, oscillator parameters and oscillator impurities that are important for quantifying the ICI effects on OFDM communication systems caused by timing jitter on receiver ADC were stated. A summary of the previous studies on phase noise, phase noise models and oscillator phase noise models was presented. The information presented here will provide the basis for the analysis and the simulations presented in Chapter 5.

Chapter 4

Inter-Carrier Inteference Effects on OFDM Systems

In the previous chapters, a large portion of the literature review was presented. This review involved information on oscillators and OFDM communication systems that is necessary to analyze the effects of timing jitter in receiver ADC sampling clocks on OFDM based communication systems.

In this chapter, a summary of existing work on the ICI caused by phase noise in OFDM local oscillators and the ICI caused by ADC sampling jitter is presented.

4.1 The ICI Effects of Local Oscillator Phase Noise on OFDM Communication Systems

In this section, the previous studies on ICI caused by the phase noise of the local oscillator driving the mixers that perform the frequency upconversion and frequency downconversion in OFDM communication systems will be reviewed.

The local oscillators causing ICI in OFDM communication systems are shown in fig. 4.1 and fig. 4.2. Notice that, the transmitter and the receiver are in zero IF configuration.

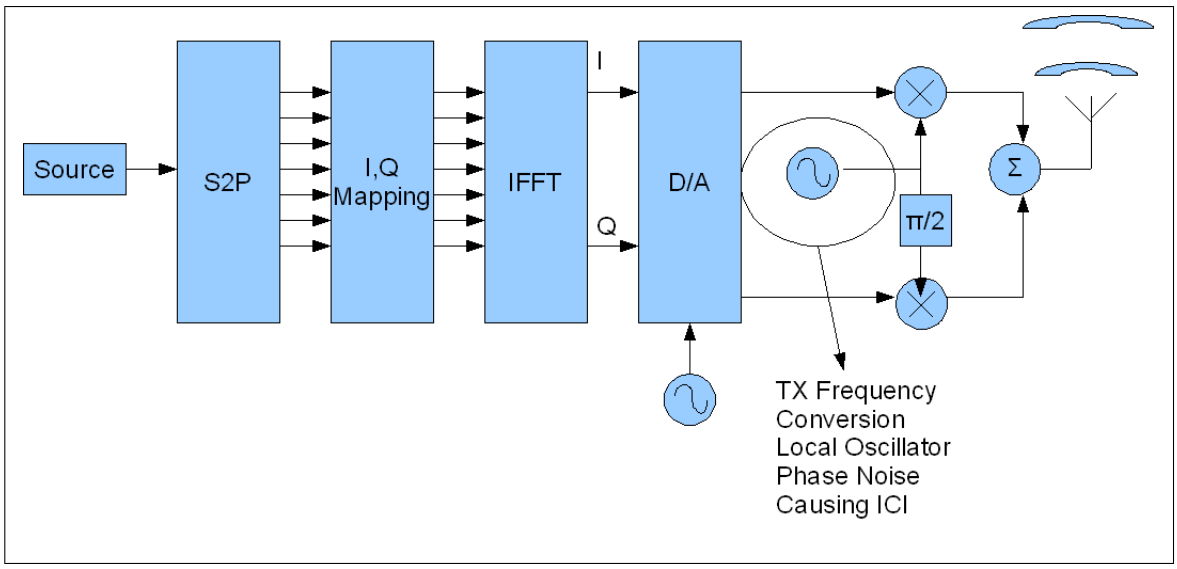

Figure 4.1: OFDM Transmitter Block Diagram Displaying the Transmit Local Oscillator Causing ICI

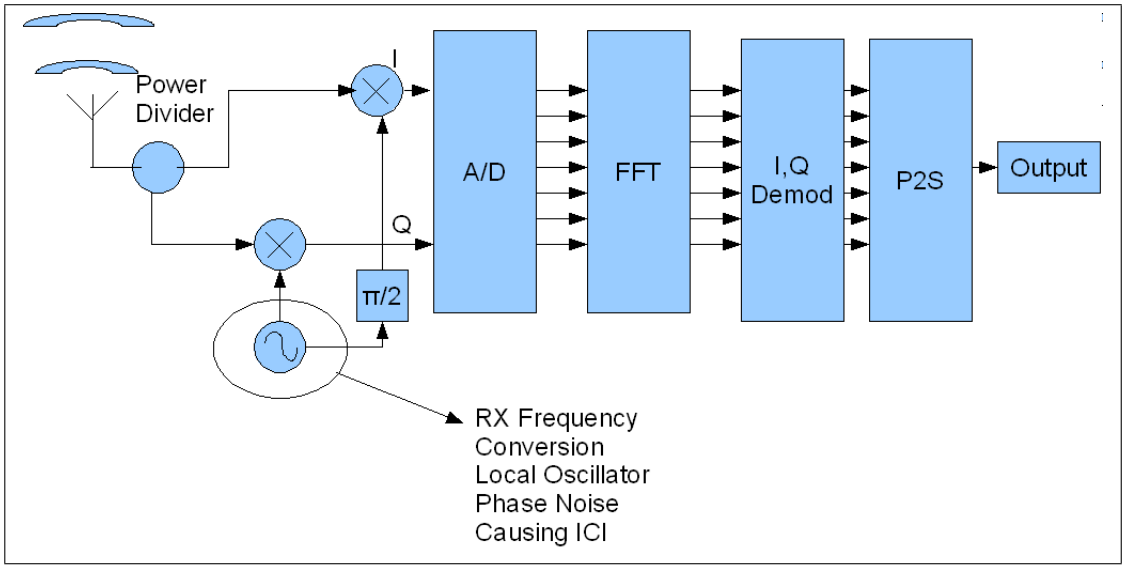

Figure 4.2: OFDM Receiver Block Diagram Displaying the Receive Local Oscillator Causing ICI

The equation for OFDM communication was given in eqn. 2.15. If there is no frequency offset between the carrier and the receiver the received signal is similar to eqn. 2.15. However, the difference between the transmitter and receiver phase noise is multiplied with the signal as shown below;

$$\tilde{x}[m] = \left\{ \frac{1}{N} \sum_{k=-\frac{N}{2}}^{\frac{N}{2}-1} \sum_{n=-\frac{N}{2}}^{\frac{N}{2}-1} (x[n] e^{j\frac{2\pi k(n-m)}{N}}) \right\} e^{j(\phi_{tr}(t)-\phi_{rx}(t))} \tag{4.1}$$

In eqn. 4.1, $\phi_{rx}(t)$ denotes the phase noise of the local oscillator at the receiver. Notice that if $n = m$ and $\phi_{tx}(t) - \phi_{rx}(t) = 0$, the OFDM system works properly. However, the phase fluctuations in the transmitter and receiver local oscillator namely, $\phi_{tx}(t)$ and $\phi_{rx}(t)$, prevent the system from having perfect synchronization. Thus, the orthogonality is degraded by the phase noise in the receiver and the transmitter. The error signal can be found by subtracting the ideal output from the output obtained in eqn. 4.1. Then, interference power in a certain OFDM channel can be calculated using the error signal shown in eqn. 4.3.

$$err(t) = \left\{ \frac{1}{N} \sum_{k=-\frac{N}{2}}^{\frac{N}{2}-1} \sum_{n=-\frac{N}{2}}^{\frac{N}{2}-1} (x[n] e^{j\frac{2\pi k(n-m)}{N}}) \right\} - \left\{ \frac{1}{N} \sum_{k=-\frac{N}{2}}^{\frac{N}{2}-1} \sum_{n=-\frac{N}{2}}^{\frac{N}{2}-1} (x[n] e^{j\frac{2\pi k(n-m)}{N}}) \right\} e^{j(\phi_{tr}(t)-\phi_{rx}(t))} \tag{4.2}$$

$$err(t) = \left\{ \frac{1}{N} \sum_{k=-\frac{N}{2}}^{\frac{N}{2}-1} \sum_{n=-\frac{N}{2}}^{\frac{N}{2}-1} (x[n] e^{j\frac{2\pi k(n-m)}{N}}) \right\} (1 - e^{j(\phi_{tr}(t)-\phi_{rx}(t))}) \tag{4.3}$$

This error consists of two parts; the first part is due to the common phase rotation in the I, Q plane. This part is caused by the mean of the error signal. This portion of the error is called Common Phase Error (CPE). The second portion is due to the varying parts of the error signal which causes power to leak between the channels. This portion of noise is the ICI.

This ICI effects can be prevented by using ICI removal algorithms at the receiver. In the next section, previous studies that have worked on the removal of these effects are reviewed.

4.1.1 Mitigation From ICI Due to Local Oscillator Phase Noise

Numerous studies have been performed to analyze the local oscillator ICI effects. Some solutions for the removal of these effects have been proposed in [23],[24].

The ICI removal algorithms depend on estimation of the phase noise waveform causing ICI and removing these effects by de-rotating the I,Q plane to compensate for the phase noise effects. The OFDM pilot signals provide a base for estimations. Since the pilot signals are signals with known content, the effects due to channel and phase effects can be estimated and compensated.

In [23], the phase noise waveform is estimated by using a Kalman filter. In this study perfect frequency and timing synchronization is assumed. In this model, the received signal is shown as in eqn. 4.4.

$$r(n) = (x(n) \otimes h(n))ej\phi(n) + \zeta(n) \tag{4.4}$$

In eqn. 4.4 $x(n)$ denotes the data that is transmitted by the transmitter, $h(n)$ denotes the impulse response of the transmission medium, $\zeta(n)$ denotes the Additive White Gaussian Noise(AWGN) in the communication system, $\otimes$ denotes circular convolution operation and $\phi(n)$ denotes the phase noise effecting the system.

After performing FFT at the receiver, the m^{th} symbol at the l^{th} channel is found as;

$$R_{m,l} = X_{m,l}H_{m,l}I_m(0) + \sum_{n=0,n\neq l}^{N-1} X_{m,n}H_{m,l}I_m(l-n) + \eta_{m,l} \tag{4.5}$$

In this equation, I_m represents the discrete spectral realization of the phase noise exponential $e^{j\phi(t)}$, during the m^{th} symbol duration.

After this characterization, the authors place a model for the phase noise function. They model phase noise by a random walk. The phase noise is generated using eqn. 4.6.

$$\phi(n) = \phi(n-1) + \omega(n) \tag{4.6}$$

Where $\omega(n)$ is a Gaussian random process with zero mean and variance $4\pi^2 f_c^2 c T_s$. Using these two models for phase noise and the OFDM system the phase noise is estimated using a Kalman filter and de-rotation is performed. Details of this algorithm can be found in [23].

In [24] the ICI effects are removed using the spectral estimates of phase noise. The communication system is modeled as done in [23]. The communication equation is as shown in eqn. 4.4. One example for the spectral estimation of phase noise is presented in fig. 4.3. The details of the estimation method can be found in [24].

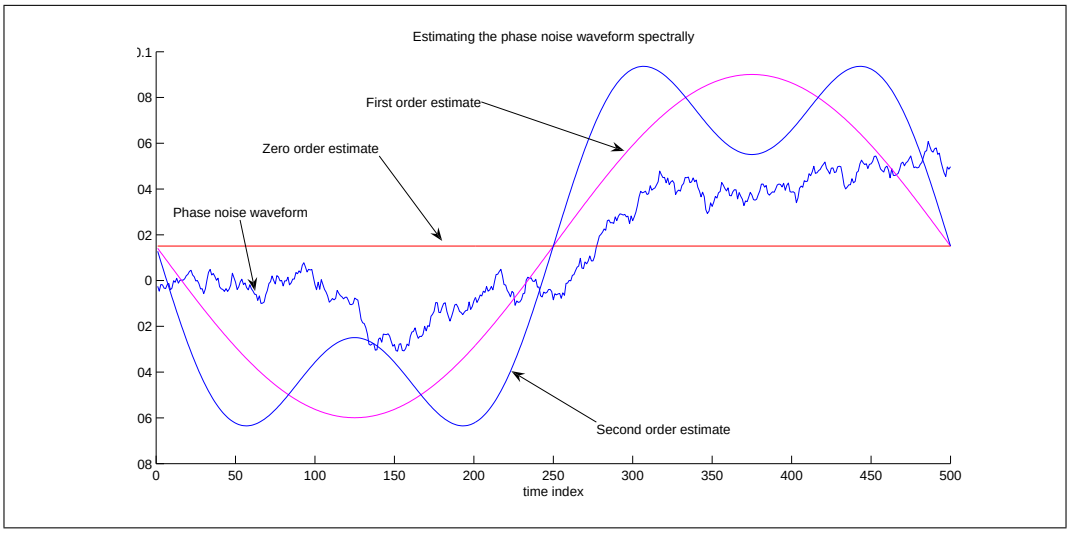

Figure 4.3: Example for Spectral Phase Noise Estimation

After the estimation of the phase noise waveform is complete, the ICI can be compensated by de-rotating the I, Q plane according to the estimates. The better the phase noise is estimated, the lower the residual ICI.

4.2 The ICI Effect Due to The Timing Jitter on Receiver ADC

In this section, a summary of the previous work on ICI caused by the timing jitter on OFDM receiver ADC's is presented. The common practice in these studies is to introduce models for OFDM systems and sampling jitter, followed by performing analysis and simulations using these models.

In [17] the OFDM system model is presented with the following equations. Equation 4.7 shows the model for the transmitted OFDM signal and eqn. 4.8 shows the signal received that is subject to sampling jitter.

$$s(t) = \sum_{k=-\frac{N}{2}+1}^{\frac{N}{2}} s_k e^{j2\pi f_k t} \tag{4.7}$$

$$s(n\Delta t + \tau_n) = \sum_{k=-\frac{N}{2}+1}^{\frac{N}{2}} s_k e^{j2\pi f_k (n\Delta t + \tau_n)} \tag{4.8}$$

As it can be seen from eqn. 4.8, this study assumes a perfect transmission medium and no other impurities except sampling jitter in the system. In the equations given above, k denotes the frequency index, n denotes the time index, Δt denotes the sampling period and τ denotes the timing jitter in sampling time.

In this study, timing jitter is assumed to be a Wide Sense Stationary(WSS) Gaussian process with zero-mean and variance, σ_j^2. Afterwards, correlation coefficients between jitter samples have been assumed. The assumed correlation coefficients (Gaussian and exponential correlation respectively) are given in eqn. 4.9 and eqn. 4.10.

$$\rho(t) = e^{-\beta^2 t^2} \tag{4.9}$$

$$\rho(t) = e^{-\alpha t} \tag{4.10}$$

Where α and β are positive numbers dictating the correlation between jitter samples.

The ICI introduced by the sampling timing jitter is calculated by performing FFT on the received signal given in eqn. 4.11 The received signal after the FFT operation is given in eqn. 4.12.

$$\hat{s}_m = \frac{1}{N} \sum_{n=-\frac{N}{2}+1}^{\frac{N}{2}} s(n\Delta(t) + \tau_n) e^{\frac{-j2\pi mn}{N}} \tag{4.11}$$

$$\hat{s}_m = \sum_{k=-\frac{N}{2}+1}^{\frac{N}{2}} s_k \left(\frac{1}{N} \sum_{n=-\frac{N}{2}+1}^{\frac{N}{2}} e^{\frac{j2\pi}{N}(k-m)n} e^{j2\pi f_k \tau_n} \right) \tag{4.12}$$

Afterwards, eqn. 4.12 is separated into two parts which show the Inter-Carrier Interference(ICI) and Common Phase Error(CPE). This bisection is shown in eqn. 4.13

$$\hat{s}_m = \eta_m s_m + \alpha_m \tag{4.13}$$

Where α_m denotes the ICI introduced and η_m denotes the common phase error. α_m and η_m are given in open form below;

$$\alpha_m = \sum_{k=-\frac{N}{2}+1, l\neq m}^{\frac{N}{2}} s_k \left(\frac{1}{N} \sum_{n=-\frac{N}{2}+1}^{\frac{N}{2}} e^{\frac{j2\pi}{N}(k-m)n} e^{j2\pi f_k \tau_n} \right) \tag{4.14}$$

$$\eta_m = \frac{1}{N} \sum_{n=-\frac{N}{2}+1}^{\frac{N}{2}} e^{j2\pi f_k \tau_n} \tag{4.15}$$

After these characterizations, ICI levels are determined by using the aforementioned characterizations on the jitter correlation $\rho(t)$. The details of the calculations and results can be found in [17].

In [18] a similar method is used for the characterization of ICI. The OFDM transmit signal is given as;

$$s(t) = \sum_{k=0}^{N-1} S_k e^{j2\pi k\Delta f t} \tag{4.16}$$

Where, s_k denotes the symbols to be transmitted and k is the carrier index.

The the signal obtained after it has been demodulated using orthogonal carriers(FFT operation) is as given below;

$$\hat{s}_k = \frac{1}{N} \sum_{l=0}^{N-1} s_l \sum_{n=0}^{N-1} e^{j\frac{2\pi(l-k)n}{N}} e^{j2\pi l\frac{\delta_n}{T}} \tag{4.17}$$

Where, δ_n denotes the jitter at the receiver sampling instant. The assumption, $\frac{\delta_n}{T} << 1$ simplifies eqn. 4.17 into the following form.

$$\hat{s}_k = \frac{1}{N} \sum_{l=0}^{N-1} s_l \sum_{n=0}^{N-1} e^{j\frac{2\pi(l-k)n}{N}} \left(1 + j2\pi l\frac{\delta_n}{T}\right) \tag{4.18}$$

Noting that the error signal is defined as $\tilde{s}_k = \hat{s}_k - s_k$ and using this information together with eqn. 4.18, the error signal due to sampling jitter at the OFDM receiver is shown below;

$$\tilde{s}_k = \frac{1}{N} \sum_{l=0}^{N-1} s_l j2\pi l \left(\sum_{n=0}^{N-1} e^{j\frac{2\pi(l-k)n}{N}} \frac{\delta_n}{T}\right) \tag{4.19}$$

After this characterization calculations on ICI are made and signal to interference ratios are calculated. Further information on the results can be found in [18].

The main difference between the aforementioned studies and the analysis presented in this thesis is the synthesis of colored jitter processes. Synthesizing receiver ADC jitter with its spectral characteristics will help quantify the ICI effect created by OFDM receiver more accurately. In [17], it is stated that Gaussian and exponential correlation functions have been assumed, because no model exists describing correlation function of jitter. This thesis does not offer a model for jitter correlation, instead ICI is calculated by generating a process that simulates the behaviour of a certain ADC circuitry.

In this chapter, the previous work on ICI effects caused by the phase noise of the local oscillators performing the frequency conversion in OFDM systems were reviewed. Also, a review of the previous work on the ICI effects due to OFDM sampling jitter was presented. These studies provide the basis for the analysis in the next chapter.

Chapter 5

Simulations on Receiver ADC Timing Jitter ICI Effects

In this chapter, the simulations that are performed for quantifying the ICI effects caused by timing jitter in OFDM receiver ADC's are presented. For performing these simulations, a simulation tool that can generate phase noise with defined spectral qualities was prepared. The MATLAB source code of this tool can be found in Appendix A. With this tool, close-in phase noise spectral density resulting from random walk in oscillator phase and the white portion of phase noise that is observed at high frequency offsets can be generated. In order to investigate the ICI effects created by the generated phase noise processes, another simulation tool that computes the ratio of the interference power to carrier power ratio created by the sampling jitter on OFDM receiver ADC was prepared. Using these two tools the ICI created by sampling jitter on OFDM receiver ADC is computed for various OFDM systems that are subject to sampling jitter with defined spectral characteristics at the OFDM receiver. Discussions are presented on the resulting ICI plots and guidelines are proposed for the design of OFDM receiver ADC circuitry.

5.1 Generating Phase Noise With Certain Spectral Characteristics

The typical phase noise spectral density of an oscillator consists of a random walk portion and a white phase noise skirt that the phase noise spectrum settles to at higher offsets, to generate this spectrum first the white noise portion of phase noise was generated. This way the spectral density of the created white phase noise can be verified analytically and the power spectral densities of the created processes can be verified.

For a generated white phase noise sequence of an oscillator at frequency f_{osc}, that has standard deviation σ_j, the power spectral density for the timing jitter can be calculated by spreading the jitter power over the Nyquist bandwidth using eqn. 5.1.

$$S_t(f) = \frac{\sigma_j^2}{f_{osc}} \tag{5.1}$$

For phase jitter the power spectral density obtained in eqn. 5.1 must be multiplied by $2\pi f_{osc}$.

$$S_\phi(f) = S_t(f) \times (2\pi f_{osc})^2 \tag{5.2}$$

Using the equations aforementioned above white phase noise was generated. The obtained power spectral density was verified. For a 250 MHz oscillator with 300 ps standard deviation, the timing jitter power spectral density can be calculated as shown below;

$$S_t(f) = \frac{\sigma_j^2}{f_{osc}} = \frac{(3 \times 10^{-13})^2}{250 \times 10^6} = 3.6 \times 10^{-}34 \tag{5.3}$$

$$S_\phi(f) = S_t(f) \times (2\pi f_{osc})^2 = 3.6 \times 10^{-}34 \times (2\pi 250 \times 10^6)^2 = 8.9 \times 10^{-}16 \simeq -150.5 dBc/Hz \tag{5.4}$$

The measured phase noise power spectral density for the sample oscillator is as depicted in fig. 5.1.

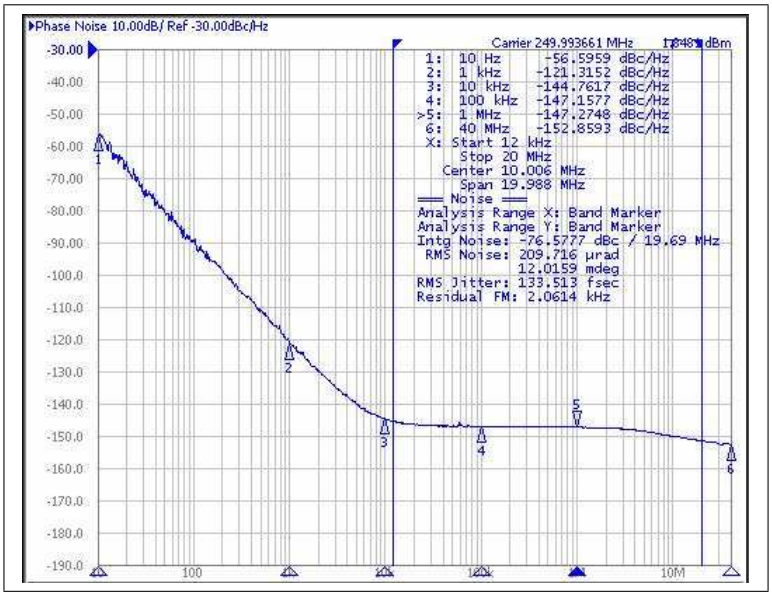

Figure 5.1: Sample Phase Noise Plot of an Vectron VCC6-QCD-250M000 Oscillator [31]

The synthesized white phase noise has the power spectral density depicted in fig. 5.2.

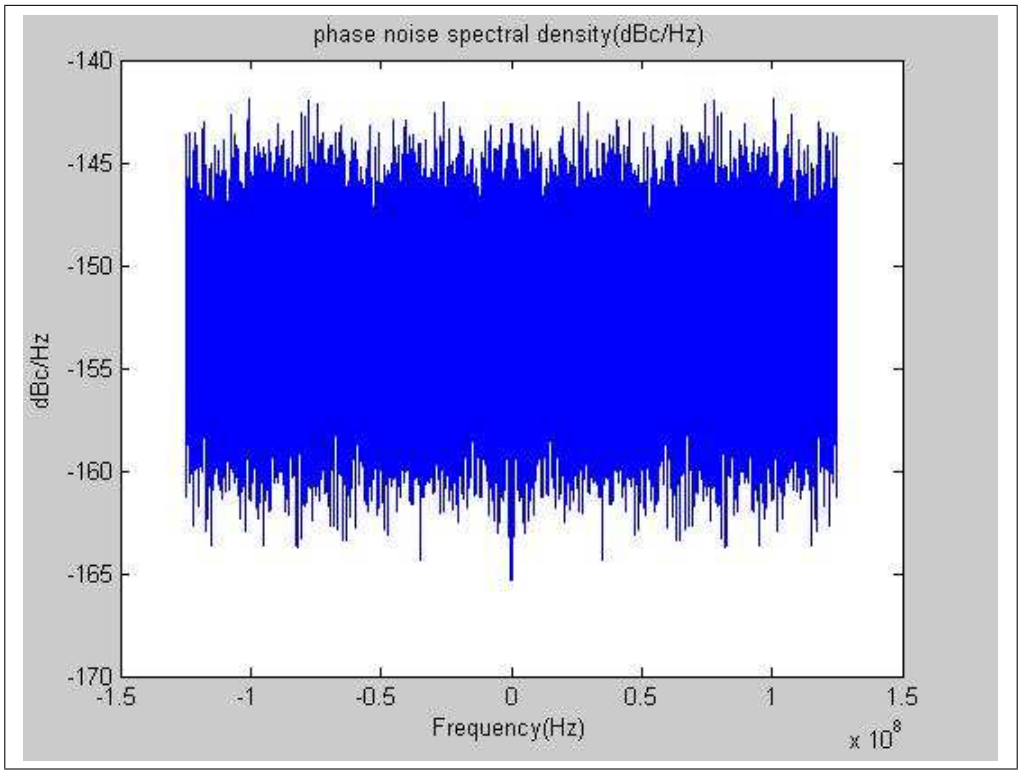

Figure 5.2: Synthesized White Phase Noise

It can be seen that the analytically determined white phase noise power level is obtained with the synthesized phase noise and it is representative of the sample oscillator depicted in fig. 5.1. Figure 5.2 is obtained by performing Monte carlo simulations that apply the Fourier transform of the autocorrelation function (Calculate the Power Spectral Density). Details can be found in Appendix A.

After being able to synthesize white phase noise with determined spectral density random walk was superposed to create a realistic phase noise spectrum. Random walk phase noise was generated using eqn. 5.5.

$$\phi[n] = \phi[n-1] + N(0, \sigma^2 2\pi f_{osc}) \tag{5.5}$$

Where, σ denotes the standard deviation of the timing jitter. After generating a jitter sequence from eqn. 5.5 the spectral characteristics of the generated process

was checked to verify the input. As stated in Chapter 3 random walk is not a Wide Sense Stationary(WSS) process. This means that, Power Spectral Density can not be computed in a straightforward manner. Still, the Fourier transform of the autocorrelation function will give a good estimate of the Power Spectral Spectral Density of the synthesized phase noise.

$$S_{\phi}(f) = \int R_{\phi}(\tau) e^{j2\pi f \tau} d\tau - (2\pi f_{osc}) \tag{5.6}$$

Equation 5.6 shows the phase noise power spectral density. In logarithmic scale the units for the output is dBc/Hz. Figure 5.3 shows the phase noise power spectral density for the synthesized phase noise

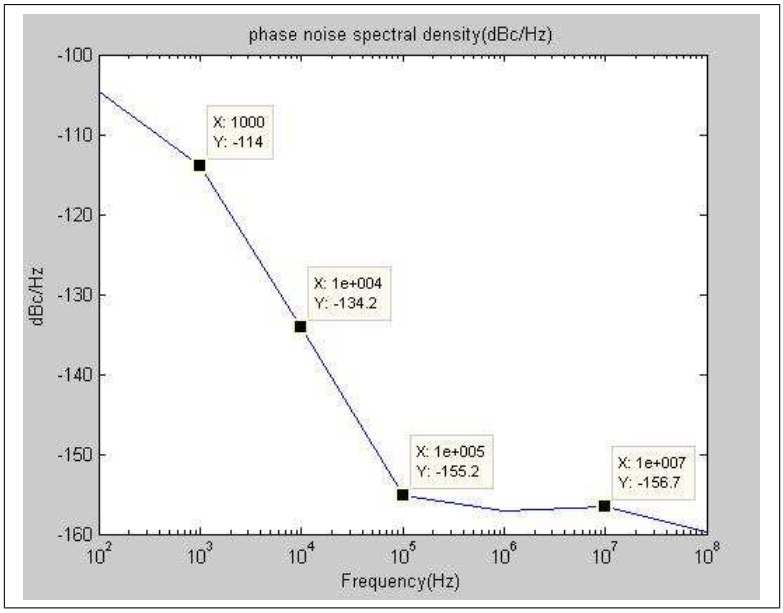

Figure 5.3: Phase Noise Power Spectral Density Created by a Random Walk with Step Strength 1fs and 400fs White Phase Noise on a 250 MHz Oscillator

In this section the method that was followed for synthesizing a realistic phase noise process was presented. The MATLAB code used for generating this process can be found in Appendix A.

5.2 Quantifying ICI Due to Timing Jitter on OFDM Receiver ADC

In order to perform simulations on the effect of timing jitter on OFDM communication systems, zero-IF transmitter and zero-IF receiver architectures were used. The channel effects were left out of the simulations by using perfect channels in the simulations. Also a perfect ADC that does not introduce quantization noise or any other additional jitter on the system is used in the simulations. Figure 5.4 depicts an OFDM receiver with timing jitter on the oscillator driving the ADC.

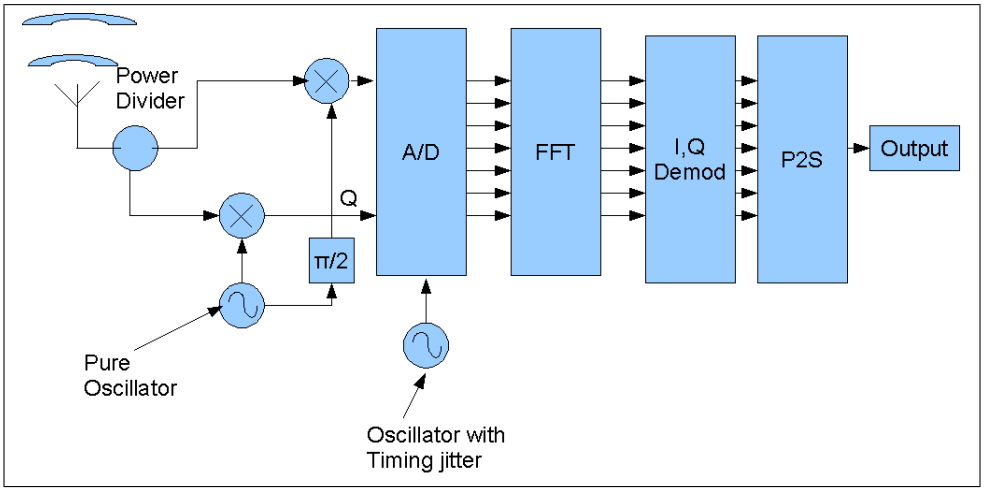

Figure 5.4: OFDM Receiver with Timing Jitter on ADC

The normalized equation for communication under the aforementioned assumptions on the system is as shown in eqn. 5.7. Notice that, the transmitted signal has no frequency or timing error until it is sampled at the receiver. The analog to digital converter sampling clock jitter distorts the timing synchronization between the carrier and the receiver, causing interference in the transmission bandwidth.

$$\tilde{x}[m] = \frac{1}{N} \sum_{k=-\frac{N}{2}}^{\frac{N}{2}-1} \sum_{n=-\frac{N}{2}}^{\frac{N}{2}} \left(x[n] e^{j2\pi \frac{(k+\zeta_k)(n-m)}{N}} \right) \tag{5.7}$$

Where, ζ_k denotes the timing jitter normalized to the sampling period T_s. Timing jitter ζ_k is a random process whose properties are defined by the oscillator driving the ADC and the ADC circuitry. Note that the timing jitter on the sampling clock distorts the received signal.

The timing jitter ζ_k, can be placed into the OFDM equations as in eqn. 5.7. Equations 5.8, 5.9, 5.10 demonstrate this using a continuous time OFDM transmit signal and eqn. 5.11 shows the discrete equivalent. In these equations, a_i and θ_i are elements from finite alphabets defining the constellation map, τ is the absolute timing jitter and ζ_k is the absolute timing jitter normalized to the sampling period.

$$x[n] = a_i e^{j\theta_i} \tag{5.8}$$

$$s(t) = x[n] e^{j\Delta\omega nt} = a_i e^{j\Delta\omega nt + \theta_i} \tag{5.9}$$

$$s(t+\tau) = a_i e^{j\Delta\omega n(t+\tau)+\theta_i} = x[n] e^{j\Delta\omega n(t+\tau)} \tag{5.10}$$

$$X[k] = x[n] e^{j2\pi(k+\zeta_k)n/N} \tag{5.11}$$

The model presented in eqn. 5.7 is sufficient for performing simulations and quantifying ICI caused by receiver ADC sampling jitter. The characteristics of jitter will effect the amount of ICI caused by the jitter on the sampling clock. In the following sections the characteristics used in simulations will be explained.

In order to perform the aforementioned ICI simulations a simulation tool that computes ICI effects due to timing jitter in the receiver ADC was prepared. With the aforementioned simulation tools, Monte Carlo simulations were performed to find an average value of ICI for each of the OFDM channels throughout OFDM transmission bandwidth. The interference power to carrier power ratio throughout the transmission bandwidth was found by computing the Mean Square Error (MSE) between the ideal received signal and dividing it to the source power. The source code for the software that is used to compute the ICI can be found in Appendix A.

$$MSE[m] = E\left[\left(x[n] - \frac{1}{N}\sum_{k=-\frac{N}{2}}^{\frac{N}{2}-1}\sum_{n=-\frac{N}{2}}^{\frac{N}{2}}\left(x[n]e^{j2\pi\frac{(k+\zeta_k)(n-m)}{N}}\right)\right)^2\right] \tag{5.12}$$

In order to separate the Intra-Carrier Interference (In-carrier Interference created in a certain carrier) created due to sampling jitter simulations were performed and the Interference caused due to single carrier is powerwise subtracted from the total mean square error obtained throughout the bandwidth. For these simulations controlled inputs (non zero inputs in single carriers) were input into the OFDM system and the Intra-Carrier Interference was calculated for all carriers. Thus the sole effect of ICI can be observed. Figure 5.5 depicts interference power to carrier power ratio caused only by Inter-Carrier Interference and interference power to carrier power ratio caused only by Intra-Carrier Interference.

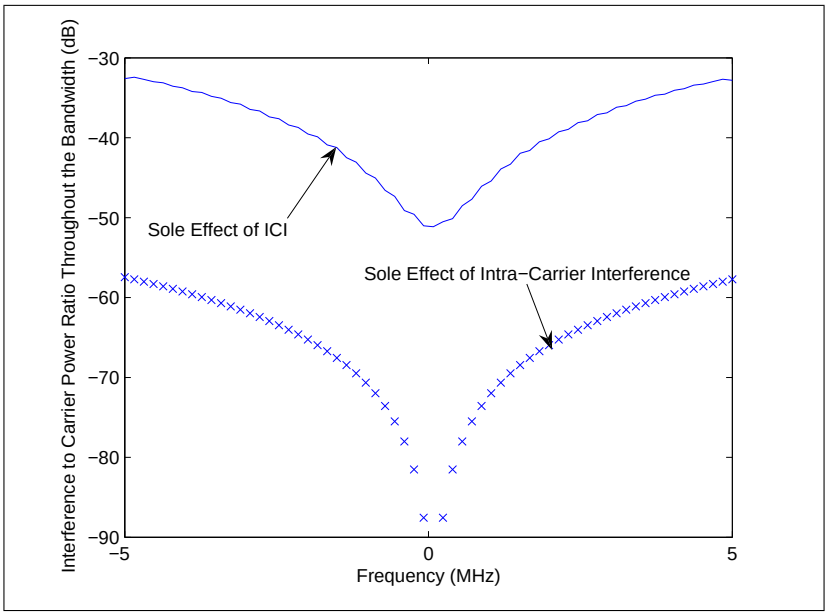

Figure 5.5: Plot Showing Interference to Carrier Power Ratios due to ICI and Intra Carrier Interference on a 4-QAM 10 MHz Bandwidth in an OFDM system with 64 Carriers having 100ps Random Walk Jitter

Figure 5.5 shows that the effect Intra-Carrier Interference is small compared to the total ICI effects that is created in a certain OFDM carrier bandwidth. Thus separating the effects does not change the total interference power to carrier power ratio drastically. Also, in designs the total interference power to carrier power ratio should be taken into consideration. In the following sections, the presented simulation results will include the total interference power to carrier power ratio.

5.3 Case Studies

In this section, the simulations and the ICI caused by jitter with defined phase noise characteristics is presented. Two OFDM based communication systems for the simulations are considered. First an IEEE 802.11a communication system with 20 MHz bandwidth and 52 carriers was considered. Second an IEEE

802.15.3a communication system is considered. This system is an UWB communication system with 500 MHz bandwidth. The bandwidth is divided into 512 channels. More details and ICI results are presented in the following subsections.

In order to quantify the ICI created in the transmission bandwidth, certain oscillators with defined phase noise characteristics are selected. Jitter processes that represent the phase noise characteristics of oscillators are synthesized and these processes are used to compute the ICI in the transmission bandwidth.

5.3.1 Case 1: IEEE 802.11a Communication System

In this case a 802.11a communication system using 4-QAM modulation on 20 MHz bandwidth and 52 carriers is considered. For the ADC, an oscillator with the phase noise spectral density depicted in fig. 5.6 is used. Oscillators with similar phase noise spectral density exist in the market and they can be used for driving an ADC.

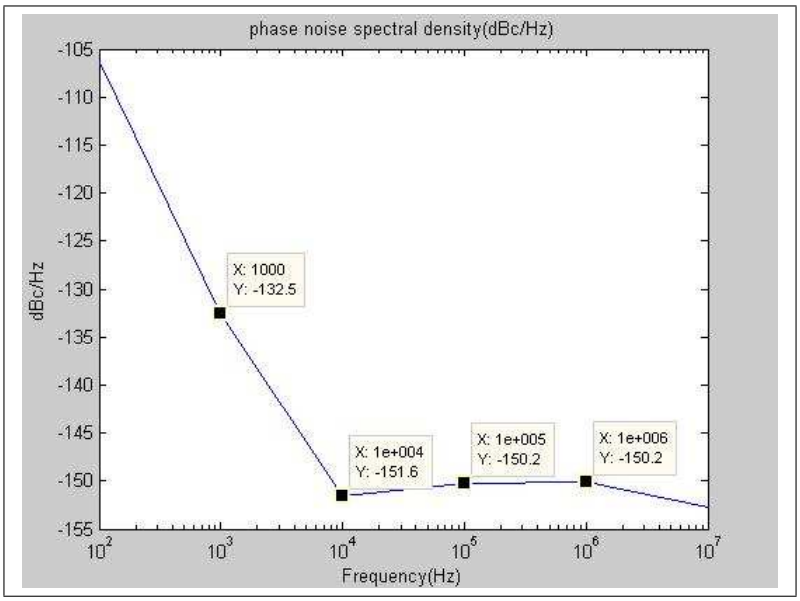

Figure 5.6: Phase Noise Power Spectral Density of Sample Oscillator 1 Used in IEEE 802.11a Simulations

The phase noise plot presented in fig. 5.6 was obtained by inputting the following parameters into the MATLAB code provided in Appendix A. Sampling period 50ns, random walk step size standard deviation of 1fs and 3ps standard deviation for the white noise.

After generating jitter with the spectral characteristics given in fig. 5.6 this jitter is injected into a 802.11a simulation and the ICI created in the OFDM carriers is obtained. The system parameters are 20 MHz system bandwidth, a total number of 52 carriers, 4 QAM constellation mapping. The resulting ICI plot is given in fig. 5.7.

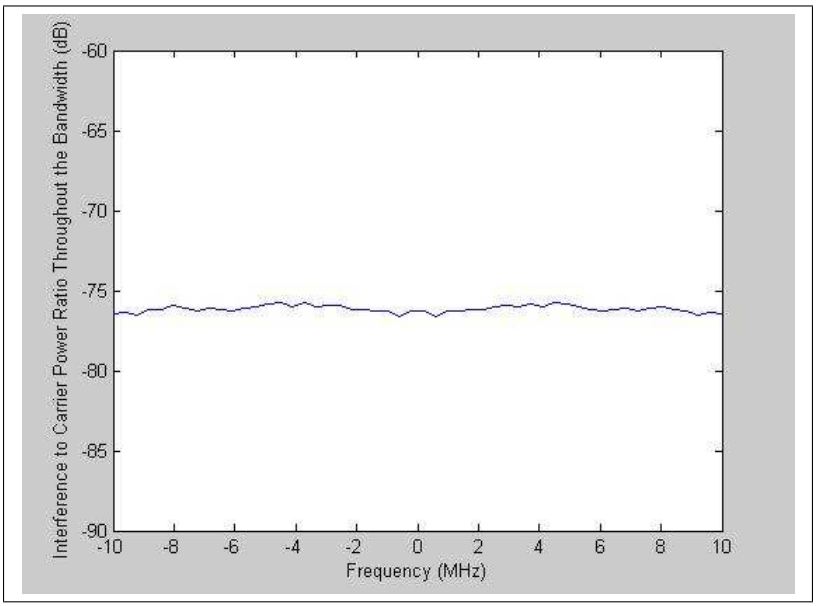

Figure 5.7: Interference to Signal Power Ratio created by Sampling Jitter on Sample Oscillator 1

It can be seen that the ICI levels introduced to the OFDM carriers are very low. This is mainly due to the superior phase noise performance of the oscillator used for driving the ADC. Figure 5.7 also shows that the created ICI levels are dominated by the white portion of the phase noise of the oscillator, fig. 5.8

depicts the ICI levels created when the ADC is driven by an oscillator that has random walk phase noise with standard deviation 3ps.

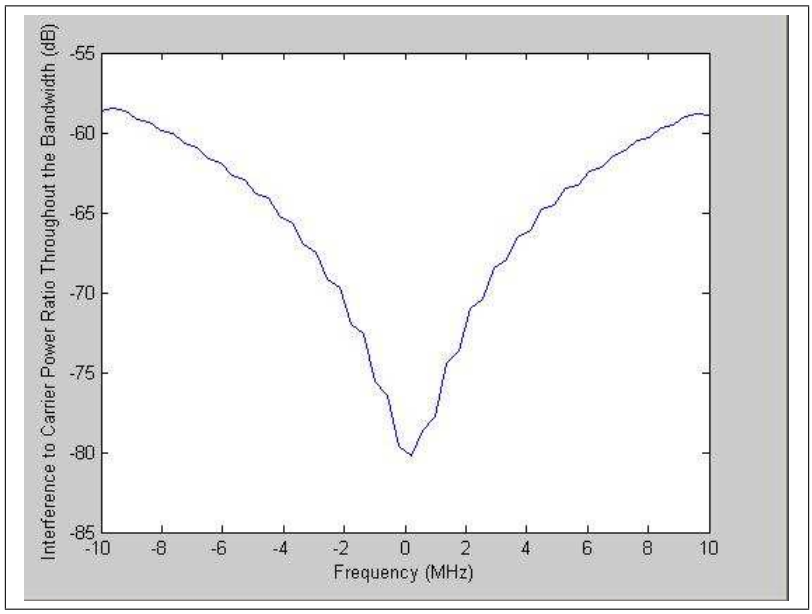

Figure 5.8: Interference to Signal Power Ratio created by Sampling Jitter on Sample Oscillator That Only has 3ps Random Walk Jitter

Figure 5.8 shows that the interference levels created by sampling jitter in OFDM receiver ADC's increase at channels with higher frequency this is mainly caused by the increase in time slope as channel frequency increases. Equation 5.13 intuitively explains this increase with the help of Taylor series expansion.

$$x(t)|_{t=t_0+\Delta t} = x(t_0+\Delta t) = x(t_0) + x'(t_0)\frac{\Delta t}{1} + x''(t_0)\frac{(\Delta t)^2}{2} + ... \qquad (5.13)$$

It can be seen that, if the time derivative of $x(t)$ is high, the deviation from the correct sampling point is high.

The ICI due to white jitter is well-spread across the spectrum, whereas ICI created due to random walk causes more ICI in the OFDM close carriers. The common feature for white jitter and random walk jitter is the ICI created by these impurities is higher at higher frequencies. Figure 5.9 depicts the interference to signal power ratio created in 10 MHz 64 Channel system when the only 10^{th} carrier is used. The random walk is created by a step standard deviation of 1 ps. Figure 5.10 and depicts the interference to signal power ratio plot when white jitter with 1ps standard deviation is injected into the same system. Figure 5.11 depicts the interference to signal power ratio created due to white jitter with standard deviation 1ps is injected into the system and the only used carrier is the first carrier.

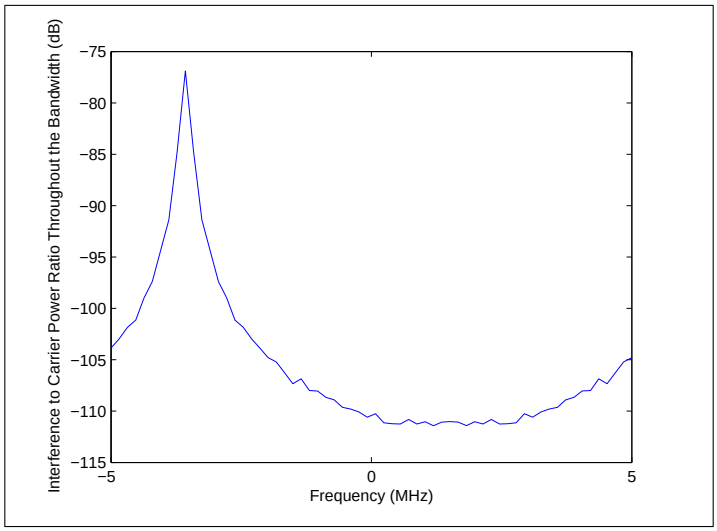

Figure 5.9: Interference to Signal Power Ratio Created by Random Walk Sampling Jitter, Only Channel 10 is Used

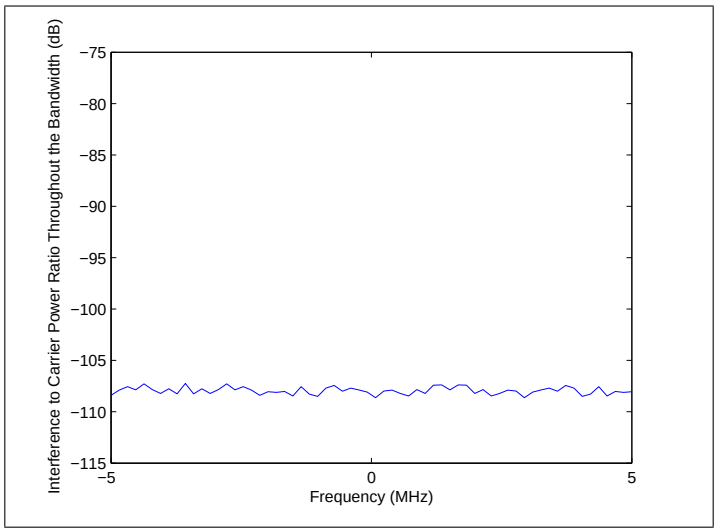

Figure 5.10: Interference to Signal Power Ratio Created by White Sampling Jitter, Only Channel 10 is Used

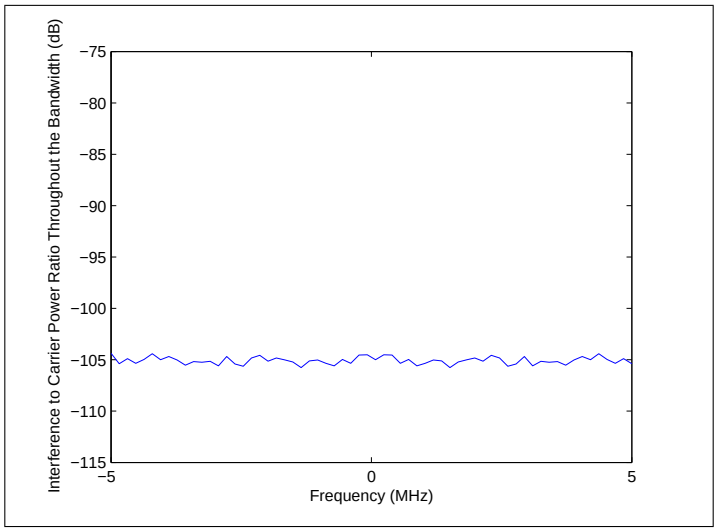

Figure 5.11: Interference to Signal Power Ratio Created by Sampling White Jitter, Only Channel 1 is Used

5.3.2 Case 2: IEEE 802.15.3a Communication System

In this section, the effect of timing jitter on receiver ADC for another communication system is quantified. This system is an Ultra Wide Band(UWB) communication system with bandwidth 500 MHz. The transmission bandwidth is divided into 512 carriers and 4-QAM constellation mapping is used. A sample phase noise waveform with the phase noise spectral characteristics depicted in fig. 5.12 is generated using random walk jitter with step standard deviation 1fs and white jitter with standard deviation 400fs.

The interference to signal power ratios at OFDM carriers are depicted in fig. 5.13

Again fig. 5.13 shows that the created ICI levels are low but it contributes to the total SINAD (Signal-to-Noise plus Distortion Ratio). When designing a

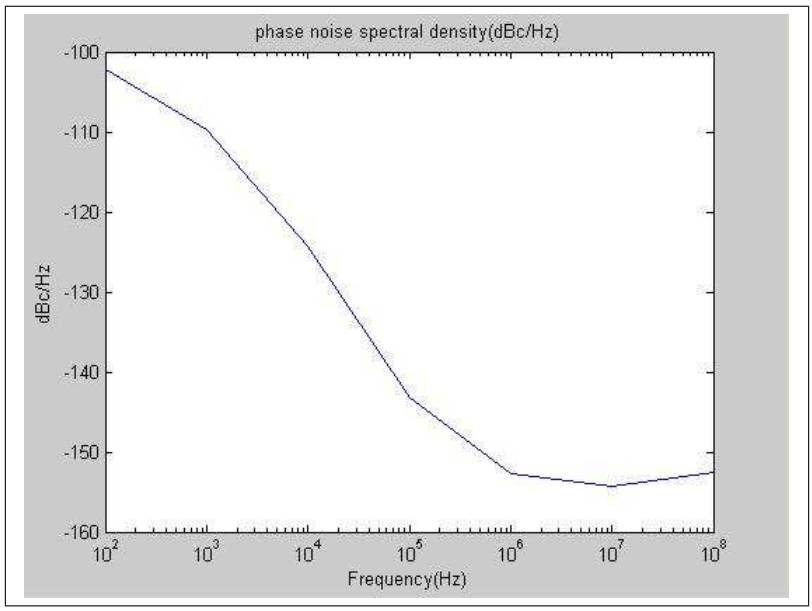

Figure 5.12: Sample 500MHz Oscillator 1 Used For Simulations of IEEE 802.15.3a UWB Communication System

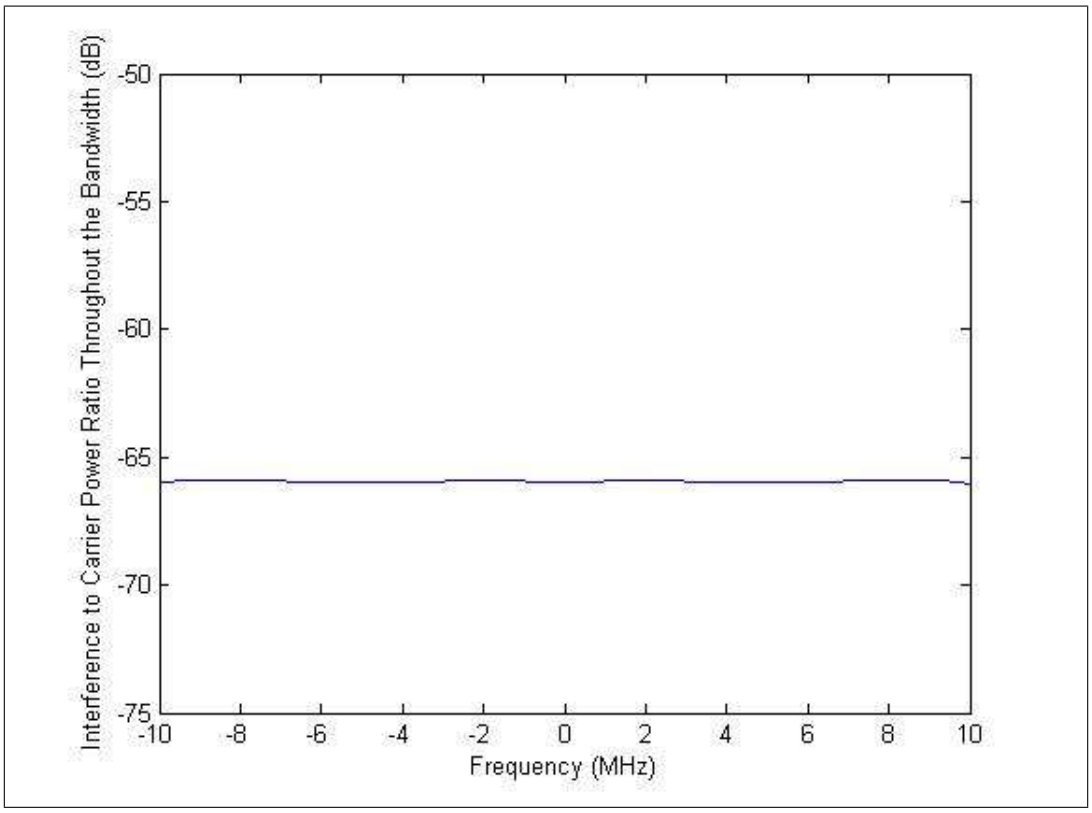

Figure 5.13: Interference to Signal Power Ratio Created by Timing Jitter Created Sample 500 MHz Oscillator 1

communication system the noise and interference levels should be distributed among contributors and components should be chosen according to this budgets.

The oscillators that were used in simulating IEEE 802 ICI levels were chosen as overtone crystal oscillators. It seems that these oscillators are over-designs for the aforementioned IEEE 802 communication systems. In order to provide and example to oscillators with inferior phase noise performance a VCO (voltage controlled oscillator) with the phase noise power spectral depicted in fig. 5.14 is input to the system and the ICI levels are calculated. The phase noise is depicted in fig. 5.14 is obtained by 0.1 ps random walk and 10 fs white phase noise.

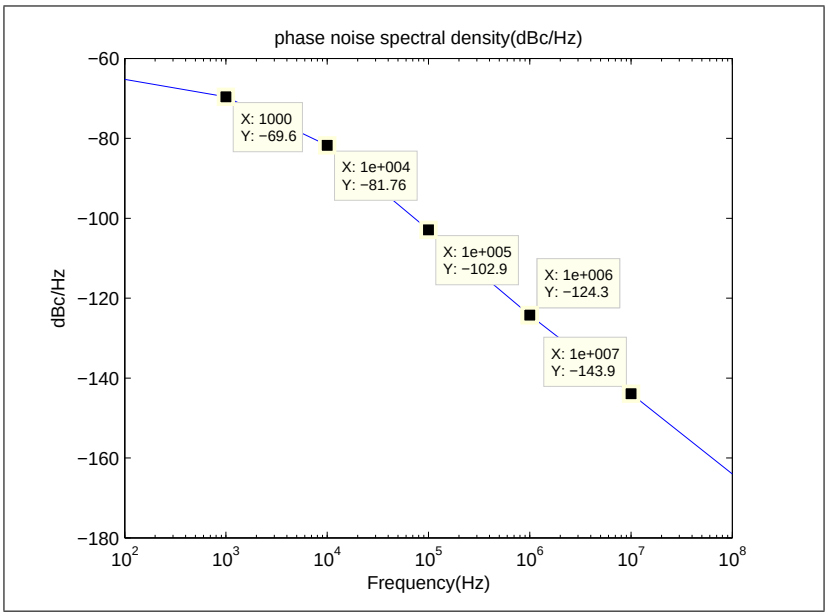

Figure 5.14: Sample 500MHz Oscillator 2 Used For Simulations of IEEE 802.15.3a UWB Communication System

The interference to signal power ratios at OFDM carriers are depicted in fig. 5.15

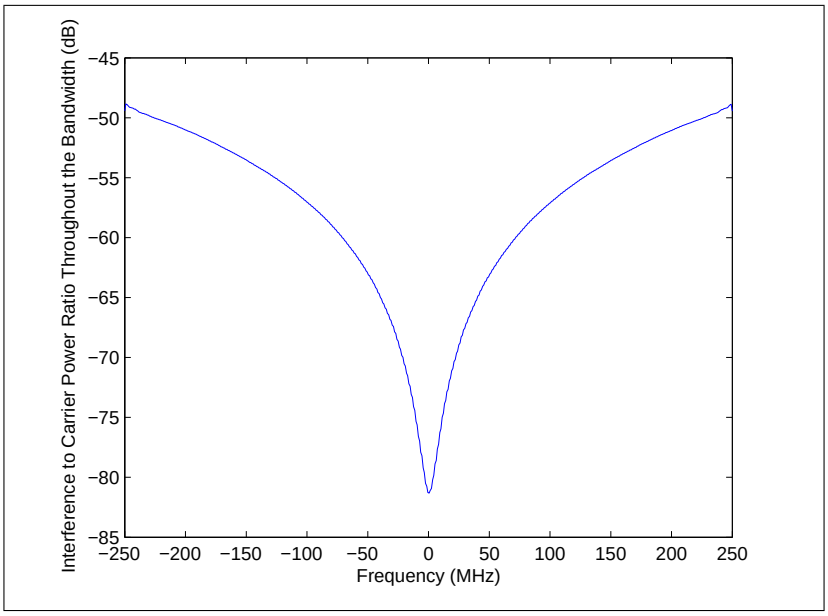

Figure 5.15: Interference to Signal Power Ratio Created by Timing Jitter Created Sample 500 MHz Oscillator 2

It is seen that the created ICI levels are higher when an oscillator with inferior characteristics is used. The interference levels created by sampling jitter are of significance to the system.

5.4 Minimum White Phase Noise in An Amplifier

In the simulations that were performed, the dominance of white phase noise characteristics on the ICI levels for certain systems was observed. Here it is just examine white phase noise, its sources and the method to calculate the power spectral density of white phase noise.

White phase noise is mainly created by the thermal noise inherent in the system. White phase noise spectral density can be calculated with the help of thermal noise floor formula. The thermal noise power spectral density available at the output of an oscillator can be calculated as follows;

$$S_w(f) = \beta kT \tag{5.14}$$

In eqn. 5.14, β is a representative figure denoting the contribution of oscillator to the white phase noise power spectral density (β is related to the resonator, the wide band power supply noise etc.), k denotes the Boltzmann constant and T denotes the ambient temperature. This equation states that, the available noise spectral density is amplified by β and raised to the level stated in eqn. 5.14. The unit for $S_w(f)$ is *Watt/Hz*, to convert the spectral density into Single Side Band (SSB) phase noise, the thermal noise spectral density should be divided by four times the carrier power, to calculate the phase disturbance caused by the quadrature component of white phase noise.

$$L(f) = \frac{\beta kT}{4P_s} \tag{5.15}$$

For an oscillator working at ambient temperature(300°K) with 10dBm output that uses an active device with noise figure 2 dB the white phase noise is calculated as shown in eqn. 5.16. Notice that FkT is divided by 1mW to convert the white power spectral density into units of dBm/Hz.

$$L(f) = \frac{\beta kT}{4P_s} = 10log10(1.58 \times 1.3810^{-}23 \times 300/10^{-3}) - 13 = -188dBc/Hz \tag{5.16}$$

5.5 Discussion on Simulations and Design Guidelines

The simulations performed in this chapter provide valuable information for the design of OFDM receiver ADC circuitry. Observing the results of the simulations presented in this chapter the following relations between the ICI levels and the system parameters can be stated.

- The ICI levels that occur due to sampling jitter in the OFDM receiver increase as the sampling jitter increases.
- The ICI levels that occur due to sampling jitter in the OFDM receiver increase as the total bandwidth of the system increases
- When random walk sampling jitter is dominant in a system, the amount of ICI created in OFDM carriers with high frequency indices increases as the frequency index increases.
- The Inter Carrier Interference caused in a carrier with high frequency index is greater than the Inter-Carrier Interference caused in a carrier with low frequency index.

Apart from the relations between system parameters the following guidelines for designing OFDM receiver ADC circuitry can be stated.

- When designing OFDM ADC circuitry, it is not sufficient to set the jitter specifications of the oscillator driving the ADC according to the Intra-Carrier Interference created by the jitter. This interference level is well below the actual interference level. In OFDM systems the interference level in a certain channel is dominated by the total sum of Interference created by neighbouring channels. In cases where white phase noise is dominant,

the ICI level in a certain carrier is almost equal to the sum of individual interference levels caused by OFDM carriers.

- When designing an OFDM ADC circuitry, the phase noise spectrum of the required oscillator (in the bandwidth of interest) can be more or less determined by the allowed interference level. The allowed interference levels should be considered while choosing the oscillator.

- Choosing an oscillator with the best phase noise spectrum will lower the ICI levels in the OFDM channels. This is a typical over-design, the right solution is to choose an (cheap) oscillator, such that the interference levels created in OFDM carriers are under the allowed limits (and perhaps leave some safety margin).

- The spectral characteristics of the created ICI levels are determined by the phase noise characteristics of the oscillator, the symbol rate in an OFDM channel and the total number of carriers. If the phase noise above the symbol rate is dominantly white, the ICI levels can be computed as if they were generated by white jitter. If the phase noise above the symbol rate the ICI levels are partly determined by random walk jitter, the ICI levels will have a V shape(the steepness of the V will be determined by the levels of random walk jitter power density and the white jitter power density) throughout the frequency domain. The tolerable ICI levels should be determined, in either case and an oscillator that fits the application should be chosen.

- The phase noise spectrum below the frequencies that correspond to the single channel symbol rate are unimportant because, the symbols are fast compared to the phase noise. The OFDM samples in a frame are collected before the low frequency portion of the phase noise spectrum manages to effect(rotate) them. Still if the detection process depends on the previous symbols (such as frequency correction loops or other symbol to symbol

processes), the lower frequency components of the spectrum should be evaluated independently.

- When using oscillators for driving ADC's components like clock buffers should not be used. If it is a must, the output of the buffer should be filtered using a narrow filter to control the amount of white phase noise introduced to the system.

In this section, relations between OFDM system parameters, jitter characteristics and ICI created by these parameters were presented. Also some guidelines for the design of OFDM receiver ADC circuitry is presented. The simulations performed in this chapter constitute the basis for these guidelines.

5.6 Additional Factor Effecting ICI

Generally sampling jitter is not only effected by the phase noise in the oscillator driving the ADC. For example ADC's add uncertainty to ζ_k. The sample and hold circuitry in the input and output of ADC's add uncertainty to the sampling instants. This uncertainty is known as "aperture jitter" and the rms value for aperture jitter is given in ADC datasheets[25].

Other circuitry(i.e clock distribution circuitry) in the path of the sampling clock signal could add jitter to the clock signal. These uncertainties should be taken into account in the design process.

Chapter 6

CONCLUSIONS

In this thesis, the effect of timing jitter on receiver ADC's on OFDM based communications systems were investigated with simulations. In these simulations, models for jitter on ADC clocks and OFDM communication systems have been used. The simulations focused on the ICI effects in OFDM carriers for ADC driver clocks with different spectral characteristics. In this respect, jitter processes with defined spectral characteristics are generated. In generating the jitter processes, oscillators from different oscillator manufacturers are considered. The spectral qualities of the generated processes are matched to the information on the datasheets of the oscillators that are considered. The noise models used in the simulations were of completely random nature. However, it is well known that a certain spectral distribution can be created by completely different time waveforms. Two different processes, with different time waveforms, could effect a system in different ways. Thus in order to synthesize a process, its nature must be taken into account. In oscillators, phase noise is mainly created due to the characteristics of the resonator, the noise of the active device (amplifier) used in the oscillator and the power supply noise. Also, buffers along the sampling clock routes introduce phase noise of random walk and white nature to the phase noise spectrum.

ICI levels due to sampling jitter in OFDM receivers can be computed more accurately by using realistic phase noise models. Realistic phase noise models also gives information on the spectral behaviour of ICI levels. Knowledge of these levels can help OFDM ADC circuitry to be designed in an efficient manner.

Respectively high ICI levels are created in OFDM systems having large number of carriers and high bandwidth. This is a major problem for UWB systems. The OFDM carriers will be subject to high ICI levels, even for very pure oscillators. Thus when implementing an OFDM based UWB communication system one might be bound to exploit the spectral behaviour of ICI. If the ICI has a V-shaped distribution, the information carried through carriers subject to high ICI could have digital modulations with less complexity (i.e using BPSK instead of 4-QAM). Thus the required SNR for the carriers subject to high ICI would reduce. This action results with increased ICI immunity in OFDM carriers with high carrier numbers.

The generated jitter processes are injected to IEEE 802.11a and IEEE 802.15.3a communication systems and the Inter-Carrier Interference levels created in OFDM are quantified for these systems. Relations between certain OFDM parameters and created ICI levels are presented. These relations state that, the ICI levels created due to sampling clock jitter in OFDM channels increase as the jitter on the sampling increases and the created ICI levels in OFDM systems increases as the total bandwidth increases.

Based on the results of the simulations, it was concluded that the ICI levels created by receiver sampling jitter in an OFDM based communication system depend on the system parameters and the spectral phase noise characteristics of the oscillator used in the ADC circuitry. Using the simulation results, some

guidelines for OFDM receiver ADC circuit design are proposed. These design guidelines are listed below;

- When designing OFDM ADC circuitry, it is not sufficient to set the jitter specifications of the oscillator driving the ADC according to the Intra-Carrier Interference created by the jitter. This interference level is well below the actual interference level. In OFDM systems the interference level in a certain channel is dominated by the total sum of Interference created by neighbouring channels. In cases where white phase noise is dominant, the ICI level in a certain carrier is almost equal to the sum of individual interference levels caused by OFDM carriers.

- When designing an OFDM ADC circuitry, the phase noise spectrum of the required oscillator (in the bandwidth of interest) can be more or less determined by the allowed interference level. The allowed interference levels should be considered while choosing the oscillator.

- Choosing an oscillator with the best phase noise spectrum will lower the ICI levels in the OFDM channels. This is a typical over-design, the right solution is to choose an (cheap) oscillator, such that the interference levels created in OFDM carriers are under the allowed limits (and perhaps leave some safety margin).

- The spectral characteristics of the created ICI levels are determined by the phase noise characteristics of the oscillator, the symbol rate in an OFDM channel and the total number of carriers. If the phase noise above the symbol rate is dominantly white, the ICI levels can be computed as if they were generated by white jitter. If the phase noise above the symbol rate the ICI levels are partly determined by random walk jitter, the ICI levels will have a V shape(the steepness of the V will be determined by the levels of random walk jitter power density and the white jitter power density) throughout the frequency domain. The tolerable ICI levels should

be determined, in either case and an oscillator that fits the application should be chosen.

- The phase noise spectrum below the frequencies that correspond to the single channel symbol rate are unimportant because, the symbols are fast compared to the phase noise. The OFDM samples in a frame are collected before the low frequency portion of the phase noise spectrum manages to effect(rotate) them. Still if the detection process depends on the previous symbols (such as frequency correction loops or other symbol to symbol processes), the lower frequency components of the spectrum should be evaluated independently.

- When using oscillators for driving ADC's components like, clock buffers should not be used. If it must the output of the buffer should be filtered using a narrow filter.

In this thesis, the focus was on the the sampling jitter effects at the receiver ADC. With the jitter effects at the receiver the OFDM symbols are detected with the addition of time lead or time lag. However, jitter at the transmitter DAC degenerates the output signal away from a sinusoidal signals. This phenomenon should be analyzed using different formulations. Intuition suggests that these effects should be symmetric for the transmitter and the receiver, (at least for small jitter approximations) but analytical formulation of this symmetry is much more difficult. Therefore, analysis is carried out only for ADC sampling jitter at the receiver and extension to DAC sampling jitter at the OFDM transmitter is left out for future work.

The future work of this study could include measurements on various OFDM systems in order to verify the models used in thesis. This can be done by comparing measured ICI levels and the simulation results. Another future could be,

simulating ICI levels caused by timing jitter in ADC sampling clock for different OFDM architectures. In this study zero-IF configurations were used. In this configuration sampling is performed at baseband. Instead, a receiver that performs sampling at some IF could be used as OFDM system architecture and a similar analysis can be performed. It could be expected that a receiver that performs IF sampling, will suffer much more from random walk phase noise as the ICI effects of random walk phase noise increases with frequency (given that other system parameters remain same). Lastly, the ICI effect caused by the timing jitter on transmitter DAC sampling clock could be investigated. Thus the sampling jitter effects in an OFDM communication systems can be better characterized.

APPENDIX A

MATLAB Code For Quantifying ICI

A.0.1 Quatifying The ICI Due to Jitter Caused by Colored Jitter in A/D

```
By Hamit Onur TANYERI 7 August 2009 This Code Quantifies the
total C/I ratio Caused by Sampling Jitter Due to a Colored
Oscillator Driving the ADC Spectrum The Inputs of the Code are;
- System Bandwidth in MHz - Total Number of Carriers - Digital
Modulation(constellation mapping) method (X-QAM) - The Number
of Carrier that are used; 1:total carrier number uses all of the
carriers - Standard Deviation of Random Walk Steps in seconds
- Defines the Spectra of the Oscillator Phase Noise Spectrum -
Standard Deviation of White Gaussian Noise in seconds - Defines
the Spectra of the Oscillator Phase Noise Spectrum -The Output is
the C/I ratio plot through the OFDM Transmission Bandwidth
```

Initializing The GUI MATLAB Generated Code

```
function varargout = JG2(varargin)
% JG2 M-file for JG2.fig
%      JG2, by itself, creates a new JG2 or
%    raises the existing singleton*.
%      H = JG2 returns the handle to a new
%     JG2 or the handle to
%      the existing singleton*.
%
%      JG2('CALLBACK',hObject,eventData,handles,...)
%     calls the local function named CALLBACK in
%    JG2.M with the given input arguments.
%
%      JG2('Property','Value',...) creates a
%    new JG2 or raises the existing singleton*.
%    Starting from the left, property value pairs are
%      applied to the GUI before JG2_OpeningFunction
%    gets called.  An unrecognized property name or
%    invalid value makes property application
%      stop.  All inputs are passed to JG2_OpeningFcn
%    via varargin.
%
%      *See GUI Options on GUIDE's Tools menu.
%  Choose "GUI allows only one
%      instance to run (singleton)".
%
%    See also: GUIDE, GUIDATA, GUIHANDLES

% Edit the above text to modify the response to help JG2
```

```
% Last Modified by GUIDE v2.5 06-Aug-2009 17:39:12

% Begin initialization code - DO NOT EDIT
gui_Singleton = 1;
gui_State = struct('gui_Name',       mfilename, ...
    'gui_Singleton',  gui_Singleton, ...
    'gui_OpeningFcn', @JG2_OpeningFcn, ...
    'gui_OutputFcn',  @JG2_OutputFcn, ...
    'gui_LayoutFcn',  [] , ...
    'gui_Callback',   []);
if nargin && ischar(varargin{1})
    gui_State.gui_Callback = str2func(varargin{1});
end

if nargout
    [varargout{1:nargout}] = gui_mainfcn(gui_State, varargin{:});
else
    gui_mainfcn(gui_State, varargin{:});
end
% End initialization code - DO NOT EDIT


% --- Executes just before JG2 is made visible.
function JG2_OpeningFcn(hObject, eventdata, handles, varargin)
% This function has no output args, see OutputFcn.
% hObject    handle to figure
% eventdata  reserved - to be defined in a future
% version of MATLAB
```

```
% handles    structure with handles and user data
% see GUIDATA)
% varargin   command line arguments to JG2 (see VARARGIN)

% Choose default command line output for JG2
handles.output = hObject;

% Update handles structure
guidata(hObject, handles);

% UIWAIT makes JG2 wait for user response (see UIRESUME)
% uiwait(handles.figure1);


% --- Outputs from this function are returned to the
% command line.
function varargout = JG2_OutputFcn(hObject, eventdata, handles)
% varargout  cell array for returning output args
% (see VARARGOUT);
% hObject    handle to figure
% eventdata  reserved - to be defined in a
% future version of MATLAB
% handles    structure with handles and
% user data (see GUIDATA)

% Get default command line output from handles structure
varargout{1} = handles.output;
```

```
function edit1_Callback(hObject, eventdata, handles)
% hObject    handle to edit1 (see GCBO)
% eventdata  reserved -
% to be defined in a future version of MATLAB
% handles    structure with handles
% and user data (see GUIDATA)

% Hints: get(hObject,'String')
% returns contents of edit1 as text
% str2double(get(hObject,'String'))
% returns contents of edit1 as a double


% --- Executes during object creation,
% after setting all properties.
function edit1_CreateFcn(hObject, eventdata, handles)
% hObject    handle to edit1 (see GCBO)
% eventdata  reserved - to be defined in
% a future version of MATLAB
% handles    empty - handles not created
%until after all CreateFcns called

% Hint: edit controls usually have
%a white background on Windows.
%       See ISPC and COMPUTER.
if ispc && isequal(get(hObject,'BackgroundColor'), get(0,'defaultUicontrolBack
    set(hObject,'BackgroundColor','white');
end
```

```
function edit2_Callback(hObject, eventdata, handles)
% hObject    handle to edit2 (see GCBO)
% eventdata  reserved - to be defined
%in a future version of MATLAB
% handles    structure with handles
%and user data (see GUIDATA)

% Hints: get(hObject,'String') returns contents of edit2 as text
% str2double(get(hObject,'String'))
% returns contents of edit2 as a double


% --- Executes during object creation,
% after setting all properties.
function edit2_CreateFcn(hObject, eventdata, handles)
% hObject    handle to edit2 (see GCBO)
% eventdata  reserved - to be defined in a future version of MATLAB
% handles    empty - handles not created
% until after all CreateFcns called

% Hint: edit controls usually have a white background on Windows.
%       See ISPC and COMPUTER.
if ispc && isequal(get(hObject,'BackgroundColor'), get(0,'defaultUicontrolBack
    set(hObject,'BackgroundColor','white');
end
```

```
function edit3_Callback(hObject, eventdata, handles)
% hObject    handle to edit3 (see GCBO)
% eventdata  reserved - to be
%defined in a future version of MATLAB
% handles    structure with
%handles and user data (see GUIDATA)

% Hints: get(hObject,'String')
% returns contents of edit3 as text
% str2double(get(hObject,'String'))
%returns contents of edit3 as a double


% --- Executes during object creation,
% after setting all properties.
function edit3_CreateFcn(hObject, eventdata, handles)
% hObject    handle to edit3 (see GCBO)
% eventdata  reserved - to be defined in a future version of MATLAB
% handles    empty - handles not
%created until after all CreateFcns called

% Hint: edit controls usually have a white background on Windows.
%       See ISPC and COMPUTER.
if ispc && isequal(get(hObject,'BackgroundColor'), get(0,'defaultUicontrolBack
    set(hObject,'BackgroundColor','white');
end
```

```
function edit4_Callback(hObject, eventdata, handles)
% hObject    handle to edit4 (see GCBO)
% eventdata  reserved - to be
%defined in a future version of MATLAB
% handles    structure with
%handles and user data (see GUIDATA)

% Hints: get(hObject,'String')
%returns contents of edit4 as text
% str2double(get(hObject,'String'))
% returns contents of edit4 as a double


% --- Executes during object creation,
% after setting all properties.
function edit4_CreateFcn(hObject, eventdata, handles)
% hObject    handle to edit4 (see GCBO)
% eventdata  reserved - to be defined
% in a future version of MATLAB
% handle empty - handles not created
%until after all CreateFcns called

% Hint: edit controls usually have a white background on Windows.
% See ISPC and COMPUTER.
if ispc && isequal(get(hObject,'BackgroundColor'), get(0,'defaultUicontrolBack
    set(hObject,'BackgroundColor','white');
end
```

```
function edit6_Callback(hObject, eventdata, handles)
% hObject    handle to edit6 (see GCBO)
% eventdata  reserved - to be defined
% in a future version of MATLAB
% handles    structure with handles
% and user data (see GUIDATA)

% Hints: get(hObject,'String') returns
% contents of edit6 as text
% str2double(get(hObject,'String'))
%returns contents of edit6 as a double



function edit6_CreateFcn(hObject, eventdata, handles)
% hObject    handle to edit6 (see GCBO)
% eventdata  reserved - to be
% defined in a future version of MATLAB
% handles    empty - handles not
% created until after all CreateFcns called

% Hint: edit controls usually have a white background on Windows.
%       See ISPC and COMPUTER.
if ispc && isequal(get(hObject,'BackgroundColor'), get(0,'defaultUicontrolBack
    set(hObject,'BackgroundColor','white');
end
function edit7_Callback(hObject, eventdata, handles)
```

```
% hObject    handle to edit7 (see GCBO)
% eventdata  reserved - to be defined
% in a future version of MATLAB
% handles    structure with
% handles and user data (see GUIDATA)

% Hints: get(hObject,'String')
%returns contents of edit7 as text
% str2double(get(hObject,'String'))
%returns contents of edit7 as a double


function edit7_CreateFcn(hObject, eventdata, handles)
% hObject    handle to edit7 (see GCBO)
% eventdata  reserved - to be
% defined in a future version of MATLAB
% handles    empty - handles not
% created until after all CreateFcns called

% Hint: edit controls usually have a white background on Windows.
% See ISPC and COMPUTER.
if ispc && isequal(get(hObject,'BackgroundColor'), get(0,'defaultUicontrolBack
    set(hObject,'BackgroundColor','white');
end

% --- Executes on button press in pushbutton1.
function pushbutton1_Callback(hObject, eventdata, handles)
% hObject    handle to pushbutton1 (see GCBO)
% eventdata  reserved - to be
```

```
%defined in a future version of MATLAB
% handles    structure with
% handles and user data (see GUIDATA)
```

—– End Of GUI Initialization

Get parametes form GUI

```
bandwidth=eval(get(handles.edit1,'String'))*1e6
numb_chan=eval(get(handles.edit2,'String'))
jitter_rw=eval(get(handles.edit3,'String'))
DMT=eval(get(handles.edit4,'String'))
full_carriers=eval(get(handles.edit6,'String'));
jitter_W=eval(get(handles.edit7,'String'))
```

– The ICI calculation Software

```
channel = numb_chan;
cons_comp=DMT;
Ts=1/bandwidth;
fc=full_carriers;
```

Loop entry condition

```
c=1;
mse_old=zeros(1,channel);
mse_cur=ones(1,channel);
hold off
```

While difference in MSE drops under some limit

```
randn('state',0); %% set seed for randn
while abs(mse_cur-mse_old)>1e-4*abs(mse_old)
    mse_old=mse_cur;
    c=c+1; % hold count
    %% create source
    source=zeros(channel,1);
    for z=1:length(fc)
        source(fc(z),1)=qammod(randint
        (1,1,cons_comp-1,0),cons_comp);
    %% set seed for rand
    end
    %% create jitter with desired spectral characteristics
    jit=zeros(1,channel);
    for z=1:channel-1
        jit(channel-z)=jit(channel-z+1)
        +normrnd(0,jitter_rw);
    end
    jit=(jit+normrnd(0,jitter_W,1,channel))/Ts;
    %% Jitter characteristics specified
    %% model - inner product
    inner_product=zeros(channel);
    N = channel;
    t=-N/2:1:N/2-1;
    f=-N/2:1:N/2-1;
    for n=1:channel % k time index
        for k=1:channel % n freq index
            inner_product(k,n)=exp(j*2*pi*f(n)*
            t(k)/channel)*exp(j*2*pi*f(n)*jit(k)/channel);
```

```
        end
    end
    inner_product2=zeros(channel);
    for n=1:channel % k time index
        for k=1:channel % n freq index
            inner_product2(k,n)=exp(-j*2*pi*f(n)*t(k)/channel);
        end
    end
    output=(1/channel)*inner_product2*(inner_product*source);
    %% Mean squared error calculation
    se=(output-source).^2;
    sq_err(:,c)=se;
    mse_cur=mean(transpose(sq_err));
    sp(:,c)=source.^2; % Signal Power
end
c
```

– ICI and In band SNR Seperation Code –%%

```
randn('state',0); %% set seed for randn
inband_snr=zeros(1,channel);
% for z=1:channel-1
%     jit(channel-z)=jit(channel-z+1)+normrnd(0,jitter_rw);
% end
% jit=(jit+normrnd(0,jitter_W,1,channel));
% for z=1:length(fc) %% Inband SNR
%calculation channel by channel -- %%
%
%     source2=zeros(channel,1);
```

```
%     source2(fc(z),1)=1;
%% -- Dirac delta input only one channel full -- %%
%     n_err_inband=ones(1,channel);
%     o_err_inband=zeros(1,channel);
%     c2=0;
%     while abs(n_err_inband-
% o_err_inband)>(1e-3*o_err_inband)
%         c2=c2+1;
%         o_err_inband=n_err_inband;
%         %% model - inner product
%         inner_product=zeros(channel);
%         N = channel;
%         t=-N/2:1:N/2-1;
%         f=-N/2:1:N/2-1;
%         for n=1:channel % k time index
%             for k=1:channel % n freq index
%                 inner_product(k,n)=exp(j*2*pi*f(n)*
% t(k)/channel)*exp(j*2*pi*f(n)*jit(k)/channel);
%             end
%         end
%         inner_product2=zeros(channel);
%         for n=1:channel % k time index
%             for k=1:channel % n freq index
%                 inner_product2(k,n)=
% exp(-j*2*pi*f(n)*t(k)/channel);
%             end
%         end
%         output=(1/channel)*inner_product2*(inner_product*source2);
%         %% Mean squared error calculation
```

```
%          se_inband=(output-source2).^2;
%          sq_err_inband(:,c2)=se_inband;
%          n_err_inband=mean(transpose(sq_err_inband));
%      end
%      inband_snr(fc(z))=n_err_inband(fc(z));
% end
%
```

Calculate and Plot C/I Ratio

```
temp5=10*log10(abs(mean(transpose(sp))));
figure
f=linspace(-bandwidth/2,bandwidth/2,
length(mse_cur));
plot(f*1e-6,10*log10(mean(abs(sq_err'))
-abs(inband_snr)/temp5))
hold on
title('MSE in OFDM Carriers due to A/D Jitter in a OFDM Comm. System')
xlabel('Frequency (MHz)')
ylabel('ICI Power Throughout the Bandwidth (dB)')
%plot(f*1e-6,10*log10(abs(inband_snr)),'x')
size(abs(inband_snr))
size(mean(abs(sq_err')))
```

A.0.2 Code Generating Phase Noise Spectrum

```
By Hamit Onur TANYERI 7 August 2009 This Code Genrates Phase Noise Spectrum
With Defined Spectral Characteristics The Inputs of the Code are; -
Sampling Rate (1/Bandwidth) Standard deviation of Random Walk Phase
Noise Standard deviation of White Noise The Output Phase Noise Plot
in Units of dBc/Hz


%-------------END-------------------%
clc
clear all
Ts=1/250e6; % Full Sampling Rate
t=Ts:Ts:0.3e-3; % Time axis for full sampling rate
N=length(t)
f=linspace(-1/(2*Ts),1/(2*Ts),length(t));
% Frequency axis for full sampling rate
t_j=zeros(1,length(t)); % Initialize timing jitter
t_j_std=0.5e-15; % strength of Random Walk Steps (Standard Deviation)
p_w=400e-15; % strength of White Noise (Standard Deviation)
c=0;
psd_old=zeros(1,length(t));
psd_new=100*ones(1,length(t));
while c<10
    c=c+1;
    psd_new=psd_old;
    for l=2:length(t)
        t_j(l)=t_j(l-1)+normrnd(0,t_j_std); %create timing jitter
    end
    t_j=t_j+normrnd(0,p_w,1,N); % add white jitter
```

```
    phi_j=2*pi*(1/Ts)*t_j; % convert to phase jitter
    r_phi=xcorr(phi_j,phi_j);
    r_t=xcorr(t_j,t_j);
    %S_phi(c,:)=abs(fftshift(fft(r_phi)))/(N);
    S_t(c,:)=abs(fftshift(fft(r_t)))/(N);

end
psd_new_t=10*log10(mean(S_t));
psd_new=psd_new_t+10*log10((2*pi*(1/Ts))^2)-10*log10(2*pi*(1/Ts));

Mean_Phi=mean(psd_new)
f=linspace(-1/(2*Ts),1/(2*Ts),length(psd_new));
figure
plot(f,psd_new)
% plot(f,psd_new_t,'r')

[v100,i100]=min(abs(f-100));
[v1k,i1k]=min(abs(f-1e3));
[v10k,i10k]=min(abs(f-10e3));
[v,i100k]=min(abs(f-100e3));
[v,i1M]=min(abs(f-1e6));
[v,i10M]=min(abs(f-10e6));
[v,i100M]=min(abs(f-100e6));
f_logp=[100 1e3 10e3 100e3 1e6 10e6 100e6];
figure
pn_logp=[psd_new(i100) mean([psd_new(i1k)
psd_new(i1k+1)]) psd_new(i10k) psd_new(i100k)
psd_new(i1M) psd_new(i10M) psd_new(i100M)];
semilogx(f_logp,pn_logp)
```

```
title('phase noise spectral density(dBc/Hz)')
xlabel('Frequency(Hz)')
ylabel('dBc/Hz')
```

Bibliography

[1] R. Lipster, "Stochastic Control Lecture Notes Lecture 3," Tel Aviv University, The Iby and Aladar Fleischman Faculty of Engineering.

[2] D. B. Leeson, "A Simple Model of Feedback Oscillator Noise Spectrum," *Proc. IEEE*, vol. 54, pp. 329-330, Feb. 1966.

[3] A. Hajimiri and T. H. Lee, "A General Theory of Phase Noise Theory in Electrical Oscillators," *IEEE Journal of Solid-State Circuits*, vol. 35, pp. 326-336, March 2000.

[4] A. Hajimiri and T. H. Lee, "Oscillator Phase Noise: A Tutorial," *IEEE Journal of Solid-State Circuits*, vol. 35, no. 3, pp. 326 -336, March 2000.

[5] A. Demir, A. Mehtora, and J. Roychowhury, "Phase Noise in Oscillators: A Unifying Theory and Numerical Methods for Characterization," *IEEE Journal of Solid-State Circuits*, vol. 35, no. 3, pp. 326 -336, March 2000.

[6] R. W. Chang, "Orthogonal Frequency Division Multiplexed Data Transmission System," *"US patent 3,448,445"*, 1966

[7] R. V. Nee and R. Prasad, "OFDM For Wireless Multimedia Communications," Artech 2000.

[8] R. W. Chang, "Synthesis of Band Limited Orthogonal Signals for Multichannel Data Transmission," *Bell Labs Technical Journal*, vol. 45, pp. 1775-1796, Dec. 1966.

[9] A. R. S. Bahai, B. R. Saltzberg, and M. Ergen, "Multi-Carrier Digital Communications: Theory and Applications of OFDM," Springer 2004.

[10] W. F. Falls, "Practical Problems Involving Phase Noise Measurement," *33rd Annual Time and Time Interval Meeting* pp. 410-416.

[11] T. Reyhan, "Telecommunication Electronics Lecture Notes," Bilkent University Faculty of Engineering

[12] G. Gonzalez, "Foundations of Oscillator Circuit Design," Artech 2007

[13] E. Rubiola, "The Basics of Phase Noise," www.rubiola.org.

[14] J. Chin and A. Cantoni, "Phase Jitter ≡ Timing Jitter?," *IEEE Communications Letters*, vol .2, no.2, Feb 1998.

[15] Y. Shen, E. Martinez, "Channel Estimation in OFDM Systems," Freescale Semiconductor Application Note 3059

[16] P. B. Hor, C. C. Ko, and W. Zhi, "*BER Performance of Pulse UWB Systems in The Presence of Colored Timing Jitter*," *Ultra Wideband Systems, 2004. Joint with Conference on Ultrawideband Systems and Technologies.*

[17] U. Onunkwo, Y. (Geoffrey) Li, and A. Swami, "Effect of Timing Jitter on OFDM-Based UWB Systems," *IEEE Journal On Selected Areas In Communications*, pp. 787-793, Apr. 2006.

[18] K. N. Manoj and G. Thiagarajan, "The Effect of Sampling Jitter in OFDM Systems," *IEEE International Conference on Communications* , vol.3, pp. 2061- 2065, 2003.

[19] "A Systematic Approach to Carrier Recovery and Detection of Digitally Phase Modulated Signals on Fading Channels," *IEEE Transactions on Communications*, vol. 31, no. 7, pp. 748-754, July 1989.

[20] S. P. Nicoloso, "An Investigation of Carrier Recovery Techniques for PSK Modulated Signals in CDMA and Multipath Mobile Environments," *MS Thesis, Virginia Polytechnic Institute and State University, The Bradley Department of Electrical Engineering*

[21] K. H. Mueller and M. Muller, "Timing Recovery in Digital Synchronous Data Receivers," *IEEE Transaction on Communications* , pp. 516-531, May 1976.

[22] IEEE Standard 1139-1999, "*IEEE standard definitions of physical quantities for fundamental frequency and time metrology - random instabilities*," 1999

[23] D. Petrovic, W. Rave, and G. Fettweis, "Phase Noise Suppression in OFDM Using a Kalman Filter," *Vodafone Chair for Mobile Communications Publications*, 2003.

[24] D. Petrovic, W. Rave, and G. Fettweis, "Phase Noise Suppression in OFDM Including Intercarrier Interference," *Vodafone Chair for Mobile Communications Publications*, 2003.

[25] W. Kester, "Aperture Time, Aperture Jitter, Aperture Delay Time - Removing the Confusion," ANALOG DEVICES Tutorial MT-007, Oct. 2008.

[26] T. Feng, H. Xianhe, W. Wei, and Fu Wei, "Analysis of Phase Noise and Timing Jitter in Crystal Oscillator," *International Conference on Communications, Circuits and Systems*, Jul. 2007.

[27] T. Pollet, M. V. Blade, and M. Moeneclaey, "BER Sensitivity of OFDM Systems to Carrier Frequency Offset and Wiener Phase Noise," *IEEE Transactions on Communications*, vol. 43, no. 4, Apr. 1995.

[28] L. Tomba and Witold Krzymien, "A Model for the Analysis of Timing Jitter in OFDM Systems," *International Conference on Communications*, vol.3, pp. 1227-1231, Jun. 1998.

[29] D. Efstathiou, "Designing clock distribution for a WCDMA transceiver system," *Fifth International Symposium Communication Systems, Networks and Digital Signal Processing*,Jul. 2006.

[30] "The Crest Factor in DVB-T (OFDM) Transmitter Systems and its Influence on the Dimensioning of Power Components" Rohde Schwarz Application Note 7TS02,January 2007

[31] "Typical Phase Noise Performance for the VCC6 series" Vectron Application Note http://www.vectron.com/